

## RESEARCH ARTICLE

# Understanding summer wind systems over the eastern Mediterranean in a high-resolution climate simulation

Melissa R. Latt<sup>1</sup>  | Assaf Hochman<sup>1,2</sup>  | Alberto Caldas-Alvarez<sup>1</sup> |  
Sebastian Helgert<sup>1,3</sup> | Joaquim G. Pinto<sup>1</sup> | Ulrich Corsmeier<sup>1</sup>

<sup>1</sup>Institute for Meteorology and Climate Research, Department of Troposphere Research (IMK-TRO), Karlsruhe Institute of Technology (KIT), Karlsruhe, Germany

<sup>2</sup>Fredy and Nadine Hermann Institute of Earth Sciences, The Hebrew University of Jerusalem (HUJI), Jerusalem, Israel

<sup>3</sup>Department 33, Landesanstalt für Umwelt Baden-Württemberg (LUBW), Karlsruhe, Germany

## Correspondence

Melissa R. Latt, Institute for Meteorology and Climate Research, Department of Troposphere Research (IMK-TRO), Karlsruhe Institute of Technology (KIT), Karlsruhe, Germany.  
Email: [melissa.latt@kit.edu](mailto:melissa.latt@kit.edu)

## Funding information

German Helmholtz Association (“Changing Earth” program); AXA Research Fund; Ministry of Science, Research and Arts; Helmholtz Association of German Research Centers, Grant/Award Number: VH-VI-527

## Abstract

Regional and local wind systems are often complex, particularly near coastal areas with a highly variable orography. Thus, the realistic representation of regional wind systems in weather and climate models is of strong relevance. Here, we evaluate the ability of a 13-year convection-permitting climate simulation in reproducing the interaction of several regional summer wind systems over the complex orography in the eastern Mediterranean region. The COSMO-CLM simulations are driven by hourly ERA-5 reanalysis and have a spatial resolution of 2.8 and 7.0 km. The simulated near-surface wind fields are compared with unique very high-resolution wind observations collected within the “Dead Sea Research Venue” project (DESERVE) and data from the Israel Meteorological Service synop network. The high-resolution COSMO-CLM simulations largely reproduce the main characteristics of the regional wind systems (Mediterranean and Dead Sea breeze, slope winds in the Judean Mountains and winds along the Jordan Rift valley), whereas ERA-5 is only able to represent the Mediterranean Sea breeze. The high-resolution simulations substantially improve the representation of regional winds, particularly over complex orography. Indeed, the 2.8 km simulation outperforms the 7.0 km run, on 88% of the days. Two mid-July 2015 case studies show that only the 2.8 simulation can realistically simulate the penetration of the Mediterranean Sea Breeze into the Jordan Rift valley and complex interactions with other wind systems like the Dead Sea breeze. Our results may have profound implications for regional weather and climate prediction since very high-resolution information seems to be necessary to reproduce the main summertime climatic features in this region. We envisage that such simulations may also be required at other regions with complex orography.

## KEYWORDS

complex orography, convection permitting, COSMO-CLM, Dead Sea, eastern Mediterranean, grid spacing, regional climate modelling, sea breeze

This is an open access article under the terms of the [Creative Commons Attribution-NonCommercial](https://creativecommons.org/licenses/by-nc/4.0/) License, which permits use, distribution and reproduction in any medium, provided the original work is properly cited and is not used for commercial purposes.

© 2022 The Authors. *International Journal of Climatology* published by John Wiley & Sons Ltd on behalf of Royal Meteorological Society.

## 1 | INTRODUCTION

Regional climate is strongly affected by the dominant wind systems, their variability and interactions with other components of the climate system. This is particularly the case in regions with complex orography affected by sea breeze like the Mediterranean area. In this region, near-surface wind systems play a central role in local air quality and regional climate conditions (Drobinski *et al.*, 2018a). Over the eastern Mediterranean, wind systems are especially important for the dispersion of air pollutants from power plants located on the Mediterranean coast (Alpert and Rabinovich-Hadar, 2003; Levi *et al.*, 2011), for the transport of ozone inland (Steinberger, 1980; Asaf *et al.*, 2011), for air quality in the Dead Sea valley (Kishcha *et al.*, 2016) and in mitigating heat stress in summer (Diffenbaugh *et al.*, 2007; Papanastasiou *et al.*, 2010).

The eastern Mediterranean is located between a temperate climate in the north and a subtropical climate in the south. During summer, an extended subtropical anticyclone (Azores) and the Persian Trough at lower levels dominate the synoptic conditions (Bitan and Sa'Aroni, 1992). This results in upper-mid-level large-scale subsidence accompanied by cool northwesterly low-level winds, often termed Etesians (Ziv *et al.*, 2004). In high summer (25 June–7 September), the Persian Trough dominates on about 82% of the days (Alpert *et al.*, 2004) and persistent hot and dry weather prevails (Ziv *et al.*, 2004; Lelieveld *et al.*, 2012; Hochman *et al.*, 2021). This period is expected to be lengthened by 2 months towards the end of the 21st century, under increased greenhouse gas concentrations (RCP8.5; Hochman *et al.*, 2018b).

In the eastern Mediterranean, thermal diurnal wind systems dominate the regional summer atmospheric circulation, due to the relatively weak synoptic-scale forcing (Bitan, 1976; Naor *et al.*, 2017). A region of particular interest is the region between the Mediterranean and the Dead Sea, where the summertime diurnal wind characteristics are influenced by the short distance to the Mediterranean Sea, the location of the Dead Sea at 430 m BSL, and more generally the complex orography of the region (Figure 1; Bitan, 1974; Hecht and Gertman, 2003; Goldreich, 2012). Therefore, the overall regional atmospheric circulation results from the interaction between several wind systems including the Mediterranean Sea breeze, the local Dead Sea breeze, slope winds in the Judean Mountains and winds along the Jordan Rift valley (Hecht and Gertman, 2003; Goldreich, 2012; Zardi and Whiteman, 2013; Metzger, 2017; Figure 1e,f). Indeed, a plethora of observational studies have described these wind systems and their potential impacts

(Ashbel and Brooks, 1939; Bitan, 1974; 1976; Hecht and Gertman, 2003; Naor *et al.*, 2017; Paperman *et al.*, 2021). For example, Alpert and Rabinovich-Hadar (2003) and Kunin *et al.* (2019) provided evidence that the eastward penetration of the Mediterranean Sea breeze front mitigates the hot and dry weather conditions prevalent during summer. Other studies have shown that the penetration of the Mediterranean Sea breeze into the Dead Sea valley leads to foehn events on 72% of summer evenings (Kishcha *et al.*, 2016; Naor *et al.*, 2017; Vüllers *et al.*, 2018; Kunin *et al.*, 2019). A realistic representation of regional wind systems is necessary for weather prediction and regional climate modelling in this region, since they also influence local near-surface conditions (Bucchignani *et al.*, 2016; Vüllers *et al.*, 2018; Drobinski *et al.*, 2018b) and therefore the quality of other model output parameters (Vautard *et al.*, 2013; Zhou *et al.*, 2016; Hochman *et al.*, 2018a).

Regional climate models (RCM) are used for weather forecasting, regional-scale climate process studies, and long-term climate simulations (Feser *et al.*, 2011; Kendon, 2014; Kotlarski *et al.*, 2014). Large international projects such as the COordinated Regional Downscaling EXperiment (CORDEX) continue to develop and apply regional climate models (Giorgi *et al.*, 2009). There is evidence that the dynamical downscaling approach can achieve improvements (Christensen *et al.*, 2007; Önl and Semazzi, 2009; Feser *et al.*, 2011; Prein *et al.*, 2013; Zollo *et al.*, 2016) depending on the experimental setup of the model, boundary conditions (forcing data), parameterizations, spatial resolution, location, the analysed model variables and the considered time scale (Rummukainen, 2010; Feser *et al.*, 2011; Kotlarski *et al.*, 2014; Di Luca *et al.*, 2015; Zollo *et al.*, 2016). High-resolution convection-permitting climate models may achieve best improvements in summer in areas with complex terrain and on small temporal and spatial scales (Prein *et al.*, 2013). Convection-permitting climate models are particularly suitable to study small-scale processes like local wind systems and the interaction of atmospheric flows with orography (Prein *et al.*, 2015). But running high-resolution models causes high computational costs (Kendon, 2014) and an increased grid spacing does not provide an added value in all aspects and locations (Vautard *et al.*, 2013; Zollo *et al.*, 2016; Akhtar *et al.*, 2018). Therefore, the added value of high-resolution simulations needs to be quantified in detail (Rummukainen, 2010), especially in regions like the eastern Mediterranean, which are challenging to model (Haslinger *et al.*, 2013; Panitz *et al.*, 2014; Zollo *et al.*, 2016; Akhtar *et al.*, 2018; Hochman *et al.*, 2018b).

Most regional climate model studies in the eastern Mediterranean predominantly focused on simulating 2 m

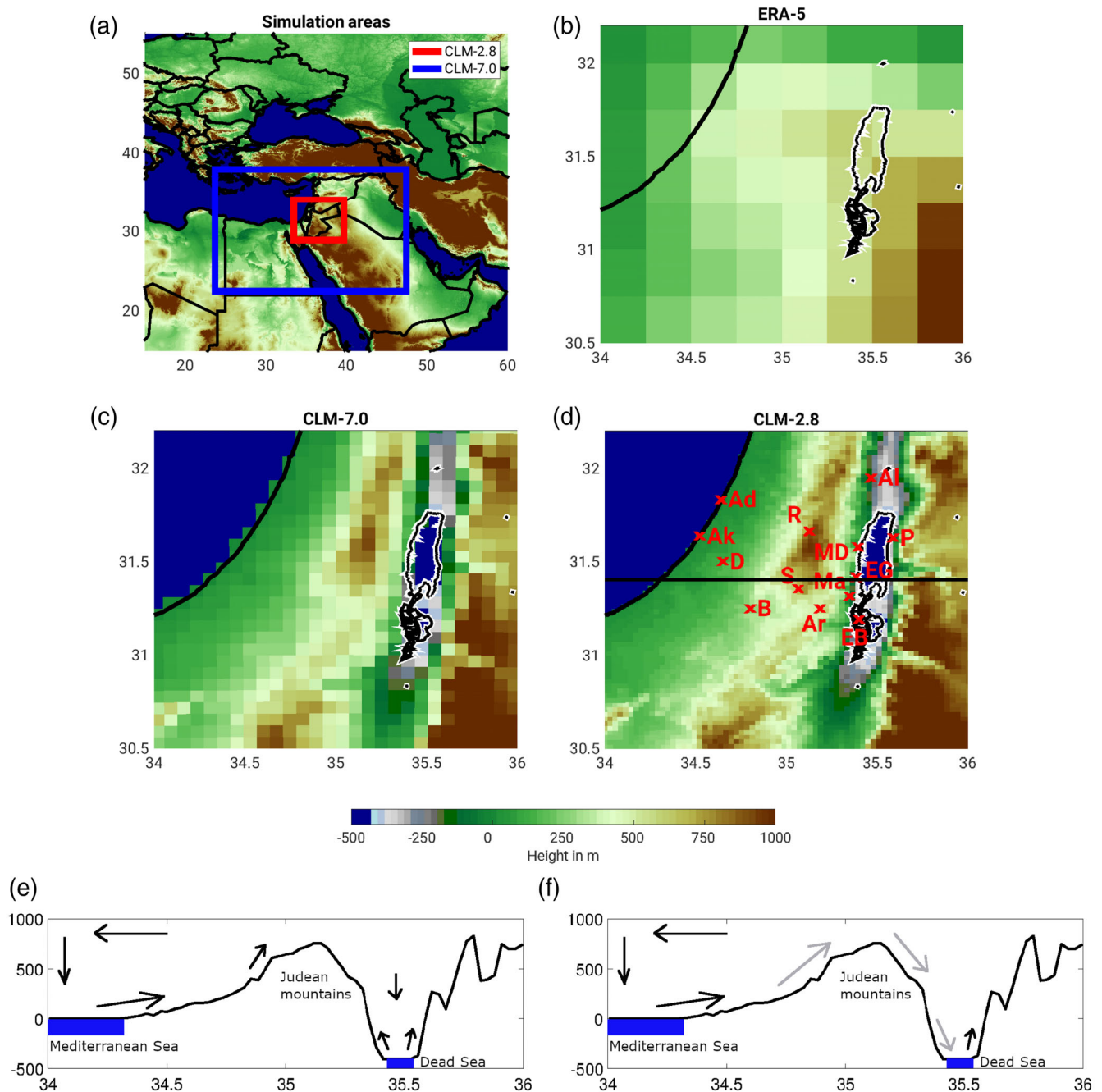


**FIGURE 1** Simulation areas of COSMO-CLM at  $\Delta x=2.8$  km (red) and  $\Delta x=7.0$  km (blue) grid spacing (a). Vertices of small red simulation area are located at  $28.92^{\circ}\text{N}$ ,  $34.04^{\circ}\text{E}$  and  $33.43^{\circ}\text{N}$ ,  $39.73^{\circ}\text{E}$ . Similarly, those of large blue area are at  $22.51^{\circ}\text{N}$ ,  $23.69^{\circ}\text{E}$  and  $37.94^{\circ}\text{N}$ ,  $47.47^{\circ}\text{E}$ . Map of model orography for ERA-5 (b), CLM-7.0 (c), and CLM-2.8 with the location of the meteorological stations (station abbreviations defined in Table 1) (d). The axes indicate latitude and longitude in degrees north and east (a–d). Schematic representation of the two sea-wind circulations of the Mediterranean and Dead Sea (e, f) along the cross-section shown as a black line in (d). The axes label longitude in degrees east and terrain height in meter ASL (e, f) [Colour figure can be viewed at [wileyonlinelibrary.com](https://onlinelibrary.wiley.com)]

temperature and precipitation (e.g., Hochman *et al.*, 2018a). Only very few modelling studies analysed wind systems in the Mediterranean region. Indeed, mostly coarse model climate simulations or high-resolution applications focused on case studies were performed (Alpert *et al.*, 1982; Alpert and Getenio, 1988;

Kishcha *et al.*, 2016; Kunin *et al.*, 2019). For example, Alpert and Getenio (1988) used a one level model with a resolution of 5 km to investigate the near-surface meso-scale flow in the Dead Sea area. In this region, high-resolution models were used to analyse wind channelling effects (Shafir *et al.*, 2008) and foehn and sea breeze

events for selected case studies (Kishcha *et al.*, 2016; Kunin *et al.*, 2019).

Motivated by the above-described gap in our understanding of wind systems and their representation in a high-resolution climate simulation, we address the following key research questions:

- Can a high-resolution model reproduce the climatology of the complex thermal summer wind systems over this region with a highly variable orography?
- Does higher resolution lead to a better statistical agreement with station data in terms of near-surface wind systems?
- Can a high-resolution model reproduce the interaction of several complex thermal summer wind systems over this region with a highly variable orography also for individual days?

The paper is structured as follows: section 2 describes the observational data sets and the model setup. Section 3 provides a climatological evaluation of near-surface wind systems (section 3.1) and a detailed analysis of two typical summer days in mid-summer 2015 (section 3.2). Section 4 summarizes and concludes the study.

## 2 | DATA AND METHODS

We use a unique set of meteorological stations operated in the framework of the DEAd SEa Research VENue

project (DESERVE, <https://www.imk-tro.kit.edu/10897.php>; Kottmeier *et al.*, 2016) (Table 1) in the fields of meteorology, hydrology and geophysics. This project aims to foster and strengthen the international and interdisciplinary scientific cooperation in the Middle East. Within DESERVE the Karlsruhe Institute of Technology (KIT) in cooperation with partners from Israel, Jordan, and Palestine among others run long-term wind measurements with sonic anemometers in high temporal resolution from 2006 to 2018 in the greater Dead Sea area at different altitudes, which allows us to identify the onset of the periodic winds for comparison with the simulations. Additionally data of eight automatic wind stations of the Israeli Meteorological Service (IMS) on a transect from the Mediterranean Sea to the Dead Sea (Table 1 and Figure 1d) were taken to complement the information for model comparison. In 2007, the IMS has transitioned all wind stations to automatic stations. The quality of the DESERVE and IMS data is tested regularly, erroneous observation periods are removed. Further outliers are detected according to the 99th percentile threshold. The 10-min wind observations are hourly averaged for comparison with the hourly model output.

The fifth generation European Center for Medium-range Weather Forecasting (ECMWF) reanalysis with a grid spacing of 0.25° (~31 km) and hourly temporal resolution was used as reference (ERA-5; Hersbach *et al.*, 2020). The ERA-5 reanalysis is considered to be particularly suitable for near-surface wind fields because compared to other common reanalysis such as the

**TABLE 1** Automatic ~10 m height wind station data over the eastern Mediterranean with the following listing columns: station name, operator, altitude, location (latitude and longitude), data availability and geographical grouping of the stations for further analyses: at the west coast of the Dead Sea (DS), in the Judean Mountains (JM) and at the Mediterranean coast (MC). Stations are operated by the Israeli Meteorological Service (IMS) and Karlsruhe Institute of Technology in the framework of the DESERVE project (KIT; Kottmeier *et al.*, 2016)

Station name	Operator	Altitude (m.a.s.l.)	Latitude (°N)	Longitude (°E)	Data availability	Grouping
En Bokek (EB)	KIT	-389	31.19	35.40	2016–2018	DS
Masada (Ma)	KIT	-7	31.32	35.35	2007–2018	
Ein Gedi Spa (EG)	KIT	-393	31.42	35.38	2014–2018	DS
Panoramic Complex (P)	KIT	+124	31.63	35.59	2014–2017	
Al-Auja (Al)	KIT	-228	31.95	35.46	2015–2018	
Ashdod (Ad)	IMS	+5	31.83	34.64	2007–2012	MC
Ashkelon (Ak)	IMS	+5	31.64	34.52	2007–2016	MC
Dorot (D)	IMS	+115	31.50	34.65	2007–2018	
Beer Sheva (B)	IMS	+279	31.25	34.80	2007–2018	
Shani (S)	IMS	+700	31.36	35.07	2007–2018	JM
Rosh Zurim (R)	IMS	+950	31.66	35.12	2007–2018	JM
Arad (Ar)	IMS	+564	31.25	35.19	2007–2018	JM
Metzoke Dragot (MD)	IMS	+20	31.59	35.39	2007–2018	

Note: Short station names refer to Figure 1d.

TABLE 2 Summary of model settings

	Resolution (°)	Grid	Convection	Turbulence	Radiation	Soil
CLM-7.0	0.0625	192 × 192 × 50	Deep and shallow (Tiedtke, 1989)	1-D TKE (Mellor and Yamada, 1974)	Ritter and Geleyn (1992)	TERRA-ML (Doms <i>et al.</i> , 2011)
CLM-2.8	0.025	120 × 120 × 60	Shallow (Tiedtke, 1989)	1-D TKE (Mellor and Yamada, 1974)	Ritter and Geleyn (1992)	TERRA-ML (Doms <i>et al.</i> , 2011)

Japanese reanalysis (JRA55) or the reanalysis 1 (R1) of the NCEP3/NCAR4, near-surface wind fields of the ERA-5 reanalysis achieve the highest agreement with global in situ observations (Ramon *et al.*, 2019).

Continuous Consortium for Small scale MOdeling in CLimate Mode (COSMO-CLM Version 5.00; Rockel *et al.*, 2008) simulations were performed for the period from 2006 to 2018 over the eastern Mediterranean (Figure 1a). The simulation period was chosen because that is the time where the most homogeneous wind observations are available for a comparison with the simulations. The regional COSMO-CLM simulations are driven by ERA-5 reanalysis. COSMO is a nonhydrostatic fully compressible atmospheric model that explicitly simulates constituents such as liquid water, dry air, water vapour and solid water on an Arkawa-C/Lorenz rotated grid (Schättler *et al.*, 2016). COSMO-CLM is the regional climate version of the Numerical Weather Prediction (NWP) model COSMO (Schättler *et al.*, 2016). COSMO-CLM has been extensively evaluated, showing good skill in representing atmospheric variables (Moemken *et al.*, 2021), also in the eastern Mediterranean (Hochman *et al.*, 2018c). The first year of simulation is removed to allow model spin up. Two COSMO-CLM simulations were performed at horizontal resolutions of 7.0 and 2.8 km, hereafter referred to as CLM-7.0 and CLM-2.8, respectively (Figure 1a). CLM-7.0 (CLM-2.8) uses 192 (120) grid points in the longitude and latitude directions and 50 (60) vertical levels (Table 2). This implies modelling the boxes 23.69°–47.47°E, 22.51°–37.94°N for CLM-7.0 and 34.04°–39.73°E, 28.92°–33.43°N for CLM-2.8. The main difference regarding physical parameterizations is the use of deep and shallow convection schemes (Tiedtke, 1989) in CLM-7.0, whereas CLM-2.8 only uses shallow convection parameterization, as deep convection in the latter is explicitly resolved. Other physical parameterizations used in CLM-7.0 and CLM-2.8 include a 1-D diagnostic closure for turbulent kinetic energy (Mellor and Yamada, 1974), grid-scale clouds and precipitation (Doms *et al.*, 2011), radiation (Ritter and Geleyn, 1992) and an 8-layer soil model called TERRA-ML (Doms *et al.*, 2011). The convection-permitting simulation (CLM-2.8) was forced by CLM-7.0, in a one-way nesting strategy. Both simulations consider a relaxation layer for

the lateral boundary conditions of 7 km. Furthermore, we dismiss four grid points at the lateral boundaries of the investigation areas to avoid possible model artefacts. Moreover, we consider tested settings for the COSMO-CLM model, which had been applied in previous studies for the eastern Mediterranean (Hochman *et al.*, 2018a,c). The COSMO-CLM model resolves the terrain well, with the 2.8 km simulation reproducing the terrain gradients even more accurately (Figure 1c,d).

The evaluation of the model results is as follows: The simulated wind fields are compared with observations at the nearest model grid point to the station of interest. We analyse noon and late evening winds, as this is the time when thermal wind systems are most pronounced due to large thermal gradients. We calculate statistical properties (mean, median, standard deviation, root-mean-square error, time lag and Pearson correlation coefficient) for hourly wind speed between 0800 and 2200 LST. In this study, all time specifications are in local summer time (LST). We use the maximum of the normalized cross correlation between the observed and modelled time series between 0800 and 2200 LST to calculate the time lag. Thus, this is the time by which the simulated time series between 0800 and 2200 LST must be shifted to achieve the maximum possible normalized cross correlation coefficient (i.e., 1) between the observed and simulated time series. The simulations are compared to observations using wind maps, diurnal cycle time series, and Taylor diagrams (Taylor, 2001). Taylor diagrams are a concise way of evaluating model data, combining several performance metrics such as standard deviation, centred root-mean-square deviation (CRMSD) and the Pearson correlation coefficient (*R*).

### 3 | RESULTS

During July and August, the synoptic conditions are persistent and the synoptic forcing is weak in the investigation area (Figure 1d). Therefore, on 95% of the summer days three thermal near-surface wind systems dominate. Starting at around 0900 LST the Dead Sea breeze, the Mediterranean Sea breeze and upslope winds in the Judean Mountains develop (Figure 1e). During the day,

the Mediterranean Sea breeze penetrates further inland and interacts with upslope winds and the Dead Sea breeze. Near the surface, upslope winds west of the Judean mountain ridge enhance the Mediterranean Sea breeze. The Dead Sea breeze and upslope winds east of the Judean mountain ridge counteract the Mediterranean Sea breeze. The extent and intensity of the Mediterranean Sea breeze is variable (Figure 1f). Three patterns are observed in the near-surface wind field during summer:

1. On most days ( $\sim 85\%$ ), the Judean Mountains are overflown and westerly winds of the Mediterranean Sea breeze replace the easterly Dead Sea breeze on the west coast of the Dead Sea (Vüllers *et al.*, 2018), hereafter referred to as a long-range wind event. It is defined as a day characterized by strong westerly wind speeds associated with the Mediterranean Sea breeze that reach far over the Dead Sea area (Metzger, 2017). This corresponds to our first case study (section 3.2).
2. On some summer days ( $\sim 10\%$ ), the Mediterranean Sea breeze does not reach the Dead Sea valley, which we refer to as a short-range wind event. This corresponds to the second case study (section 3.2).
3. On a small number of days ( $\sim 5\%$ ), the typical thermal wind systems cannot be easily identified as synoptic large-scale winds dominate.

### 3.1 | Climatology of near-surface winds in summer

In this section we evaluate the ability of COSMO-CLM simulations to reproduce summer near-surface regional wind systems in the eastern Mediterranean from a climatological perspective. The reader is referred to Video S1, Supporting Information for the averaged full diurnal evolution of wind fields in the CLM-2.8 simulation. This video shows the thermal wind systems (Figure 1e,f) described above.

From here on, COSMO-CLM 12-year mean diurnal cycles of near-surface winds are discussed chronologically from the Mediterranean coast to the Dead Sea. At 1200 LST, both COSMO-CLM simulations realistically capture the wind speed and wind direction of the Mediterranean Sea breeze near the coast ( $\sim 5 \text{ m s}^{-1}$ ) and the upslope winds ( $\sim 4 \text{ m s}^{-1}$ ) in the Judean Mountains (Figure 2c,e). At this time of the day the near-surface wind fields of the two COSMO-CLM simulations are very similar and match the observations. However the westerly wind direction is reproduced qualitatively better by the CLM-2.8 simulation. The Mediterranean Sea breeze is also represented in ERA-5 at 1200 LST, but clearly underestimated by  $\sim 2 \text{ m s}^{-1}$ , mainly due to the fact that

the simulated diurnal cycle of the wind speed is shifted about 1 hr later (Figure 3b). Upslope winds in the Judean Mountains are not represented in ERA-5, which results in an underestimation of wind speed in this region by  $\sim 2 \text{ m s}^{-1}$  (Figures 2a and 3c). Wind directions are qualitatively well simulated, except for some regions surrounding the Dead Sea. Indeed, ERA-5 is not able to represent the local Dead Sea breeze (Figure 2a). However, both COSMO-CLM simulations do reproduce the Dead Sea breeze (Figure 4a,c). In general, wind speed and direction are well reproduced by both COSMO-CLM simulations. In this regard, the wind direction in the Jordan Rift valley is qualitatively better simulated by the CLM-2.8 simulation (Figure 4a,c).

Horizontal thermal gradients are mostly small until midday, thus the wind speed is relatively low for most areas (Figure 3). In addition, small-scale features do not yet have large influence on the near-surface wind field. As a result, both simulations realistically reproduce the wind field at the Mediterranean coast and in the Judean Mountains despite different model horizontal resolutions, until that time of day. As the day progresses, horizontal pressure and temperature gradients rapidly increase and the near-surface circulation is now strongly thermally driven. At this time, small-scale features play a larger role. Therefore, the horizontal resolution of the model starts influencing the ability to simulate the wind fields (Figures 2d,f and 3).

At 1800 LST the Mediterranean Sea breeze and the upslope winds in the Judean Mountains are decreasing and turn typically clockwise to the northwest (Figures 2 and 3b,c) (Kusuda and Alpert, 1983). Further inland, on the west coast of the Dead Sea, wind speed increases and reaches its maximum of  $4.8 \text{ m s}^{-1}$  at 2000 LST (Figure 3d). The COSMO-CLM-7.0 simulation clearly overestimates wind speed at the Mediterranean coast by  $\sim 3 \text{ m s}^{-1}$  and in the Judean Mountains by  $\sim 2 \text{ m s}^{-1}$  (Figure 2d). In addition, the mean diurnal cycle of wind speed is simulated 3.5 hr (2.7 hr) too late on the Mediterranean coast (Judean Mountains; Figure 3b,c). This makes the differences between observed and simulated wind speed even larger, later in the evening. Due to the time lag and the positive bias, at the Mediterranean coast and in the Judean Mountains the correlation of the CLM-7.0 wind speed is relatively low ( $R < 0.42$ ) and the CRMSD is comparatively high ( $> 2.4 \text{ m s}^{-1}$ ; Figure 5b,c).

The CLM-2.8 simulation captures the wind speed near the Mediterranean coast and in the Judean Mountains more realistically than CLM-7.0 (Figure 2d,f). Indeed, CLM-7.0 overestimates wind speed by 63% near the Mediterranean coast, whereas CLM-2.8 only overestimates it by 13%. Moreover, the time lag of the mean diurnal cycle of wind speed in the CLM-2.8 simulation is

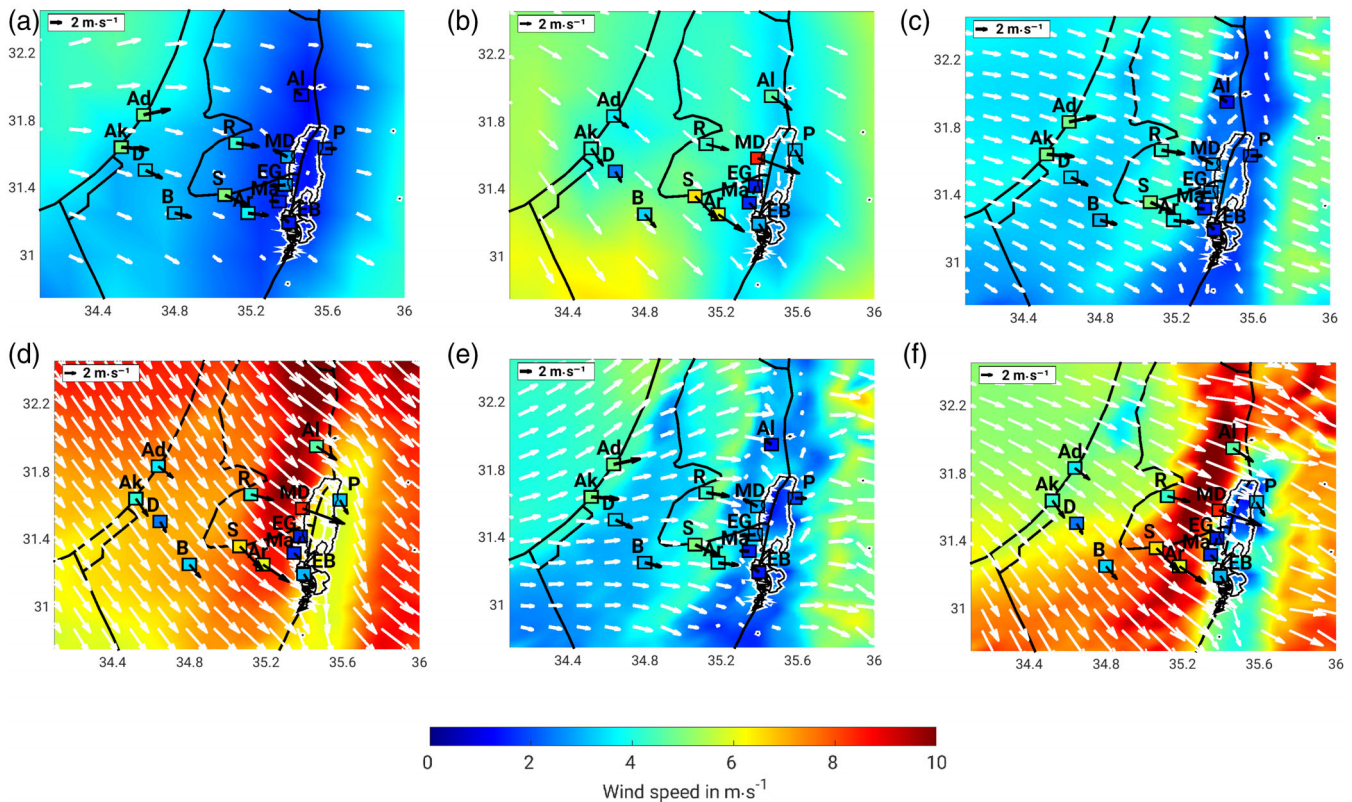


**FIGURE 2** Summer (July and August) average (2007–2018) of modelled near-surface wind fields for ERA-5 (a, b), CLM-7.0 (c, d) and CLM-2.8 (e, f) at 1200 LST (a, c, e) and 1800 LST (b, d, f). Black framed squares and black wind arrows represent observations from automatic 10 m height wind stations. White arrows show the simulated wind field. Station abbreviations are defined in Table 1. The axes indicate latitude and longitude in degrees north and east [Colour figure can be viewed at [wileyonlinelibrary.com](http://wileyonlinelibrary.com)]

much smaller than in CLM-7.0, being 1 hr on the Mediterranean coast and 1.3 hr in the Judean Mountains (Figure 3b,c). This leads to high correlation coefficients ( $R > 0.6$ ) and low CRMSD ( $< 1.8 \text{ m} \cdot \text{s}^{-1}$ ; Figure 5b,c). Near the Mediterranean coast, the ERA-5 reanalysis reproduces the strength and direction of the wind well, but the upslope winds in the Judean Mountains and wind speed near the Dead Sea, especially in Metzoke Dragot (MD), are underestimated (Figure 2b). On the other hand, both COSMO-CLM simulations do capture wind speed and direction in Metzoke Dragot (Figure 4b,d). Further down the slope, there are major differences between the two CLM simulations, as only the CLM-2.8 simulation represents a clear wind front on the west coast of the Dead Sea. As a result, wind speed on the west and east coast of the Dead Sea is only satisfactorily reproduced by the CLM-2.8 simulation and is generally overestimated by the CLM-7.0 simulation ( $> 4 \text{ m} \cdot \text{s}^{-1}$ ). In the Judean Mountains, CLM-7.0 (CLM-2.8) also overestimates wind speed by 38% (20%). In the evening, wind speed and wind direction at Rosh Zurim (R), Ein Gedi (EG), Masada (Ma), En Bokek (EB) and Panoramic Complex (P) are more realistically simulated by the CLM-2.8 simulation.

Overall, on the west coast of the Dead Sea the diurnal variation of wind speed is very well reproduced by the CLM-2.8 simulation (Figure 3d). CLM-7.0 (CLM-2.8) overestimates wind speed by 168% (48%). Indeed, the CLM-2.8 simulation is closest to observations at the west coast of the Dead Sea (Figure 5d).

Averaged over the whole area, the CLM-7.0 simulation roughly reproduces the course of the mean diurnal wind speed cycle (Figure 3a). However, wind speeds are simulated about 2 hr too late and are overestimated by  $4.3 \text{ m} \cdot \text{s}^{-1}$  at 1900 LST. This leads to a low (high) correlation coefficient (centered root mean square deviation) of  $R = 0.36$  (CRMSD =  $2.6 \text{ m} \cdot \text{s}^{-1}$ ; Figure 5a). Nevertheless, in the Dead Sea area the CLM-7.0 simulation still achieves better results than the ERA-5 reanalysis in terms of the correlation coefficient (Figure 5d). Considering all the available data, CLM-2.8 simulates the diurnal wind speed about 1 hr too late and overestimates wind speed up to  $2.1 \text{ m} \cdot \text{s}^{-1}$  at 1900 LST (Figure 3a). The largest overestimation of wind speed is found for the Judean Mountains and at the west coast of the Dead Sea. This suggests that the wind speed bias is mainly influenced by the complex orography. Our analysis regarding the bias is based

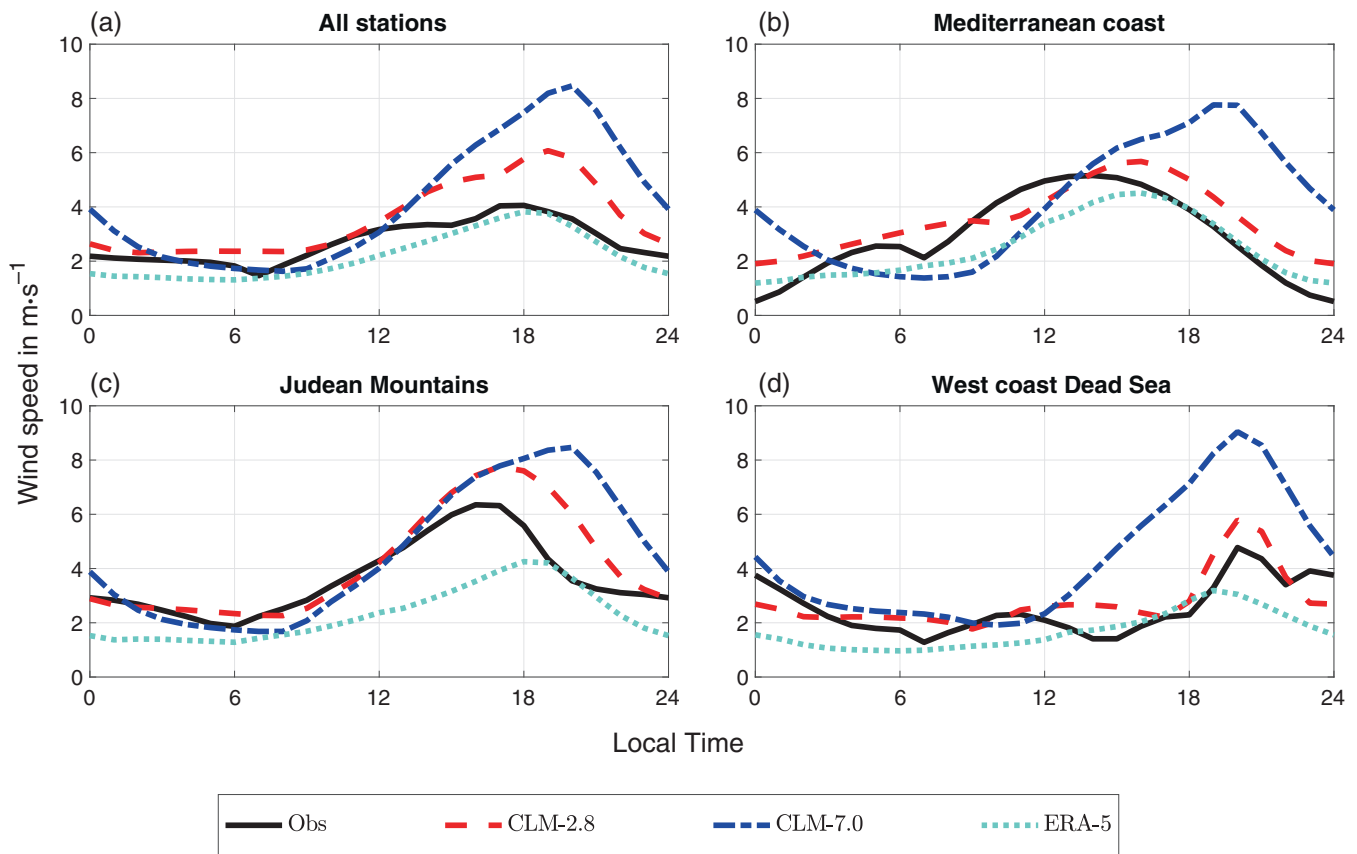


**FIGURE 3** Summer (July and August) mean diurnal cycles (2007–2018) of hourly averaged wind speed of the wind stations (Obs) and the nearest grid point of the two CLM simulations and ERA-5 reanalysis averaged for all stations (a), the Mediterranean coast (b), the Judean Mountains (c) and the west coast of the Dead Sea (d). Table 1 shows which stations belong to the different subareas [Colour figure can be viewed at [wileyonlinelibrary.com](https://onlinelibrary.wiley.com)]

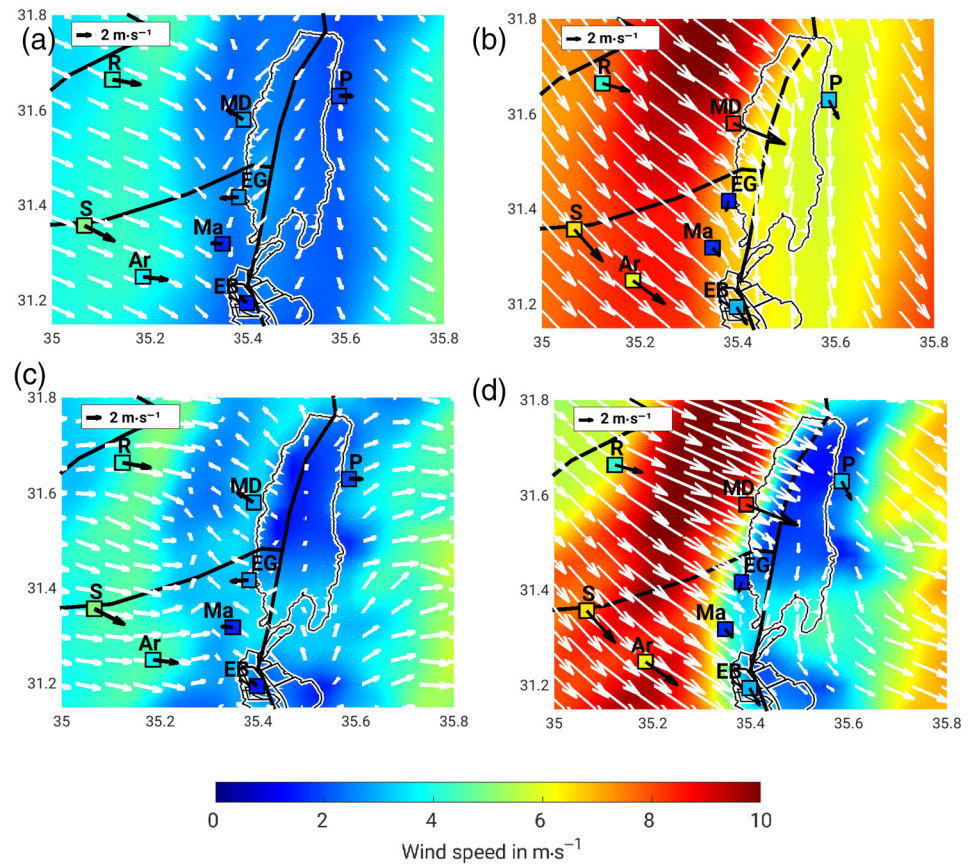
on a comparison between station observations and the closest grid point in the model. In areas with complex orography with high wind variability, a one-point wind measurement is not necessarily representative for a  $2.8 \text{ km} \times 2.8 \text{ km}$  model grid box, which represents an area average. Vice versa is also true. While the increased resolution of 2.8 km decreases the wind speed offset compared to the resolution of 7.0 km, it is still too coarse to capture in full the local small-scale wind variability. A further factor lies on the fact that some stations which are not part of the subarea analysis (e.g., Dorot and Beer Sheva) but do contribute to the overall average (Table 1 and Figure 3a) are at locations surrounded by buildings, which leads to a higher wind drag compared to the other stations.

Figure 6 shows a comparison between daily statistical properties of CLM-7.0 and CLM-2.8 for hourly wind speed during July and August of 12 years (2007–2018; 744 days). The correlation coefficient ( $R$ ) (Figure 6a,b), the root-mean-square error (RMSE; Figure 6c,d) and the difference of standard deviations (diff.  $SD$ ; Figure 6e,f) and medians (diff. median; Figure 6g,h) between observed and simulated wind speed are considered. The

left column of the figure (Figure 6a,c,e,g) shows daily mean statistical properties for hourly wind speed averaged over all wind stations, whereas, the right column (Figure 6b,d,f,h) shows the same statistical properties for selected subregions including the Mediterranean coast (blue circles), Judean Mountains (black squares) and Dead Sea (red stars).

The CLM-2.8 simulation performs better than CLM-7.0 for most summer days. In particular the correlation coefficient (RMSE) is higher (lower) for CLM-2.8 on 97% (98%) of the days compared to CLM-7.0 (Figure 6a,c). In addition the difference between observed and simulated standard deviation (median) is lower for CLM-2.8 on 95% (94%) of the summer days compared to CLM-7.0 (Figure 6e,g). Finally, on 88% of the days all four considered statistical properties suggest that CLM-2.8 performs better than CLM-7.0. Indeed, there is not even one single day that  $R$ , RMSE, diff.  $SD$ , and diff. median suggest that CLM-7.0 performs better (Figure 6a,c,e,g). However, it should be noted that both simulations tend to overestimate wind speed (Figure 6g) and its standard deviation (Figure 6e).

**FIGURE 4** As Figure 2 only for the Dead Sea area and the two CLM simulations [Colour figure can be viewed at [wileyonlinelibrary.com](https://onlinelibrary.wiley.com)]



The results averaged over all stations are mirrored by the sub-regional ones (Figure 6b,d,f,h). The largest improvements in  $R$  and RMSE are achieved by CLM-2.8 on the Mediterranean coast (Figure 6b,d). On the other hand, the statistical properties of both simulations vary the most on the west coast of the Dead Sea (Figure 6b,d,f,h). This may be due to the interaction of multiple wind systems over the complex orography near the Dead Sea, resulting in highly variable near-surface winds and very different model results.

Qualitatively and quantitatively, CLM-2.8 achieves most realistic wind speeds over the Judean Mountains, on the west coast of the Dead Sea and on average over all stations (Figures 2, 5a,c,d and 6). Furthermore, CLM-2.8 obtains very good results along the Mediterranean coast, where there is the largest improvement compared to CLM-7.0 (Figures 2d,f and 5b-d). However, the CLM-2.8 simulation tends to slightly overestimate wind speeds and to simulate the diurnal cycle 1 hr too late. But bias and time lag are smaller than in CLM-7.0. This agrees with Akhtar *et al.* (2018) as they also found that the COSMO-CLM model tends to overestimate wind speed in Israel, but this can be greatly reduced by higher model resolution, especially around the Mediterranean coast. As discussed above, the orography and surface drag could be reasons for the overestimation of wind speeds, as the

surface drag in models is often smaller than under real conditions (Nolan *et al.*, 2014). In addition, a part of the positive wind speed bias could also be related to the already known positive altitude-dependent bias of daily mean and maximum temperatures in COSMO-CLM (not shown; Kotlarski *et al.*, 2011; 2014; Cattaneo *et al.*, 2012; Panitz *et al.*, 2014; Örol and Semazzi, 2009), which leads to unrealistically large temperature gradients and thus to too intense winds. Also sea surface temperatures are subject to major uncertainties in the model boundary conditions (Evans *et al.*, 2004).

All in all, COSMO-CLM performs well in reproducing the near-surface climatological wind fields. Especially near the Mediterranean coast and in the Jordan Rift valley, where the influence of local effects is large, there are clear benefits of the high-resolution in reproducing the structure of small-scale winds (Figures 2 and 5).

### 3.2 | Near-surface winds in mid-summer case studies

In this section, the near-surface wind field of the COSMO-CLM simulations is evaluated for two selected case studies in 2015, due to data availability (Table 1). It cannot be assumed a priori that the model can both

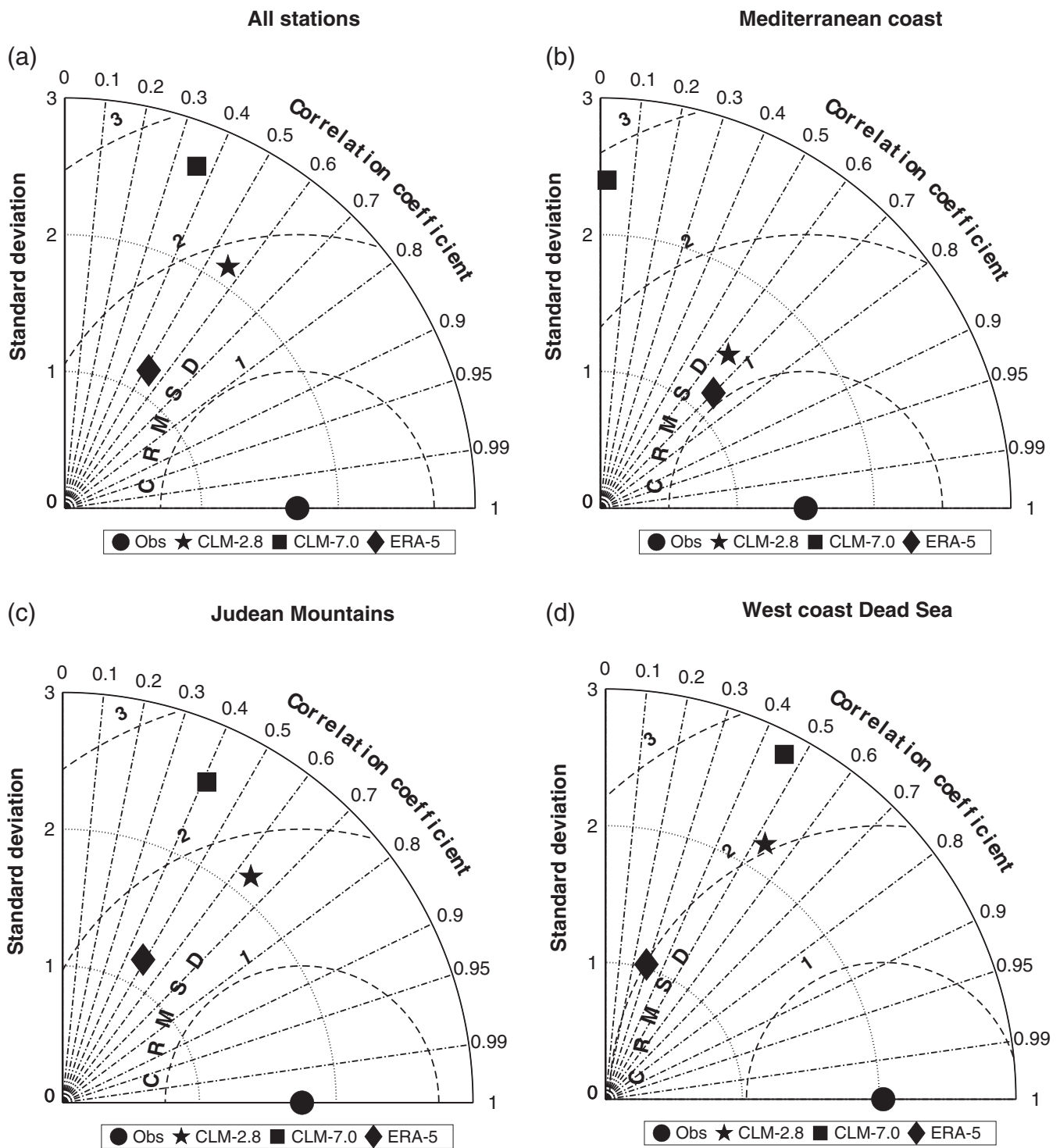


**FIGURE 5** Taylor diagrams (Taylor, 2001) for the evaluation of hourly average wind speed between 0800 and 2200 LST in July and August (2007–2018) for the two CLM simulations and the ERA-5 reanalysis regarding 10m height wind station observations (Obs) averaged for all stations (a), the Mediterranean coast (b), the Judean Mountains (c) and the west coast of the Dead Sea (d). Table 1 shows which stations belong to the different subareas

adequately represent the smoothed climatology and the individual events. Therefore, we have selected July 16, 2015 and August 3, 2015 as representative examples for a long- and a short-range wind event (see section 3 for

definition). These provide detailed insight of the wind systems.

In general, the wind fields on July 16, 2015 largely mirror the climatological daily cycle (section 3.1).

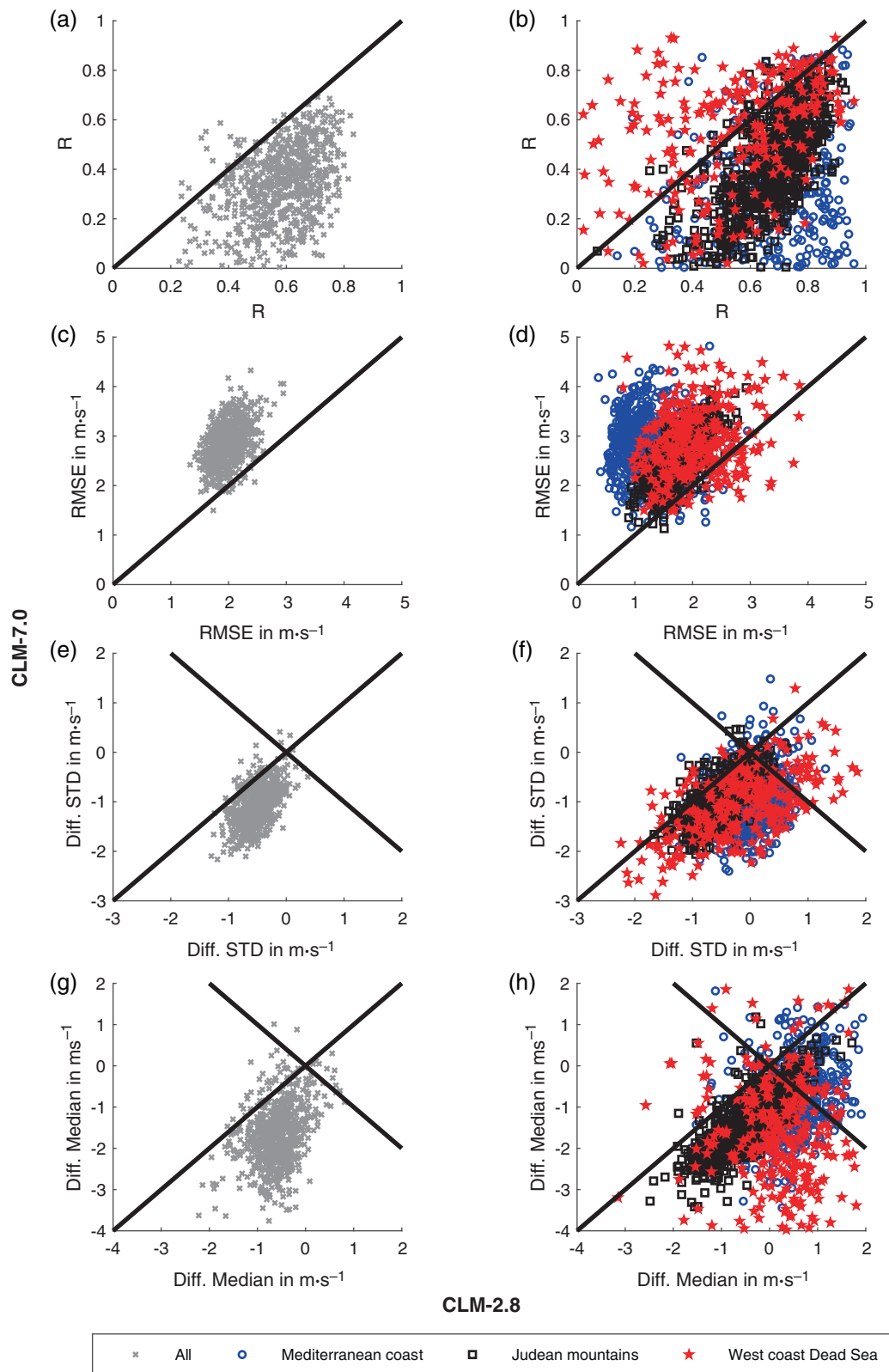


**FIGURE 6** Scatter diagrams for daily averaged statistical key figures of hourly wind speed between 0800 and 2200 LST for CLM-7.0 and CLM-2.8: Pearson's correlation coefficient (a, b), root-mean-square error (c, d), difference between observed and simulated standard deviation (e, f) and median (g, h). Left column is averaged over all stations, right column for subareas. Table 1 shows which stations belong to the different subareas. The black line separates areas where the respective statistical ratio is in favour of one of the simulations [Colour figure can be viewed at [wileyonlinelibrary.com](http://wileyonlinelibrary.com)]

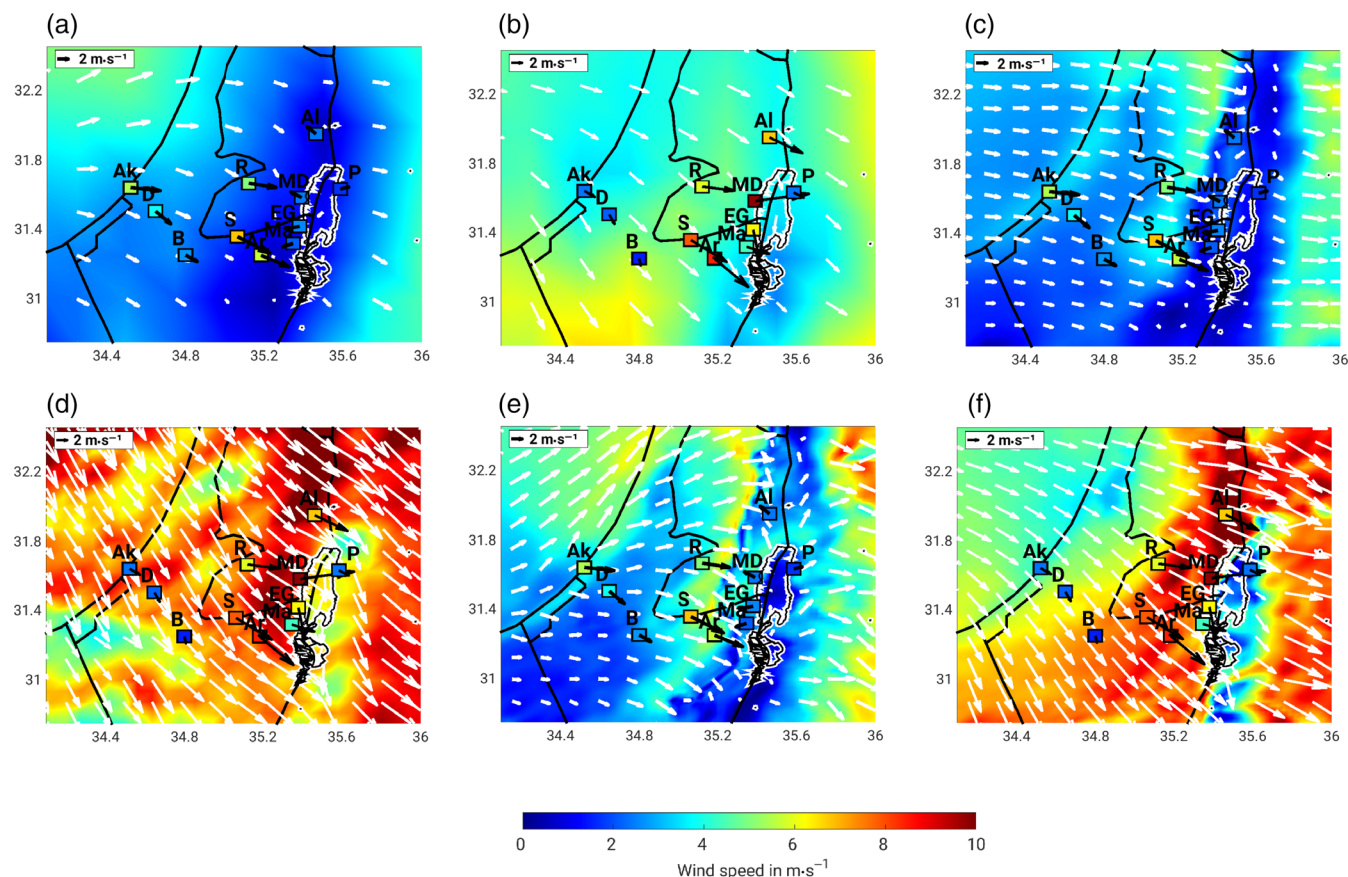


**FIGURE 7** Modelled near-surface wind fields on July 16, 2015 for ERA-5 (a, b), CLM-7.0 (c, d) and CLM-2.8 (e, f) at 1200 LST (a, c, e) and 1800 LST (b, d, f). Black framed squares and black wind arrows represent observations from automatic 10m height wind stations. White arrows show the simulated wind field. Station abbreviations are defined in Table 1. White arrows show the simulated wind field [Colour figure can be viewed at [wileyonlinelibrary.com](http://wileyonlinelibrary.com)]

During the day, the Mediterranean Sea breeze, the local sea breeze of the Dead Sea, upslope winds in the Judean Mountains and north winds along the Jordan Rift valley develop (Figures 1e,f and 7). The Mediterranean Sea breeze penetrates into the Jordan Rift valley to the west coast of the Dead Sea where it reaches its maximum wind speed of  $8.8 \text{ m}\cdot\text{s}^{-1}$  (climatology =  $4.8 \text{ m}\cdot\text{s}^{-1}$ ) at 2200 LST (2000 LST; Figures 1f and 8d). All wind systems are represented by the COSMO-CLM simulations (Figure 7c–f), but the ERA-5 reanalysis does not detect the local Dead Sea breeze, winds along the Jordan Rift valley or slope winds in the Judean Mountains (Figure 7a,b). Furthermore, also in the case study both CLM simulations mostly overestimate the wind speed, whereas ERA-5 underestimates it (Figure 8).

Our selected case studies show important features that are smoothed out in climatology. For July 16, 2015 the interaction of the different wind systems in CLM-2.8 is shown in Video S2 for the whole day. Several interactions on small scales are only reproduced in CLM-2.8. For example, at 1200 LST the convection-permitting

CLM-2.8 simulation can precisely simulate a convergence line directed north–south over the Judean Mountains that is much less resolved in CLM-7.0, but matches with observations. In the case study (Figure 9c) at the western slope of the Judean Mountains northwesterly winds up to  $7 \text{ m}\cdot\text{s}^{-1}$  are simulated, while at the eastern slope southeasterly winds of about  $5 \text{ m}\cdot\text{s}^{-1}$  are predominant. In the centre of the convergence the wind speed is reduced to  $1\text{--}2 \text{ m}\cdot\text{s}^{-1}$ , resulting in upward vertical motion (not shown). Looking at the same situation in the climate run (Figure 4c), the wind speed difference at both sides of the convergence line is much smaller and the convergence zone itself is broader. This results in less vertical motion and subsequently less convection. Convergence lines over the Judean Mountains are common features in the area and can lead to local cloud cover in summer. As may be expected, the near-surface wind field on July 16, 2015 exhibits more variability than the climatology in both observations and simulation results. As a result, there are already larger differences in the simulated wind speed at 1200 LST (Figure 7c,e) than in the climatology (Figure 2c,e).

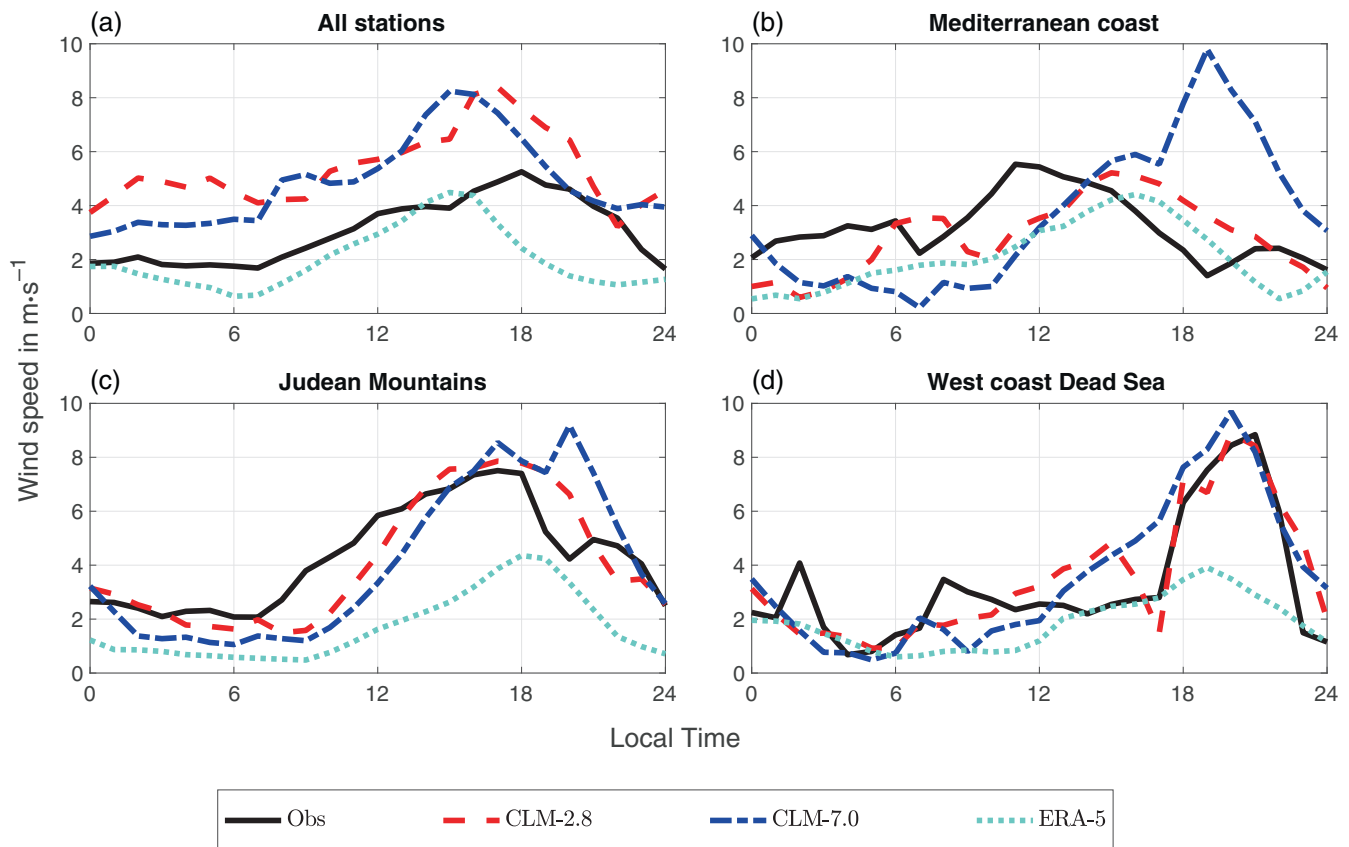


**FIGURE 8** Diurnal cycle of hourly averaged wind speed on July 16, 2015 of the wind stations (Obs) and the nearest grid point of the two CLM simulations and ERA-5 reanalysis averaged for all stations (a), the Mediterranean coast (b), the Judean Mountains (c) and the west coast of the Dead Sea (d). Table 1 shows which stations belong to the different subareas. The letters indicate the main and second maximum of the diurnal wind speed cycle for the observations (A and B) and CLM-7.0 (C and D) [Colour figure can be viewed at [wileyonlinelibrary.com](http://wileyonlinelibrary.com)]

Near the Mediterranean coast, the diurnal cycle of wind speed on July 16, 2015 has two wind speed maxima (A and B; Figures 3b and 8b). In our case study, both CLM simulations can reproduce both wind speed maxima. However, the amplitude of the first CLM-7.0 relative wind speed maximum (C) overestimates the amplitude of the observed relative maximum (A) only by  $\sim 2.5 \text{ m}\cdot\text{s}^{-1}$ . The second simulated CLM-7.0 main wind speed maximum (D) overestimates the observed main maximum (B) by  $\sim 4 \text{ m}\cdot\text{s}^{-1}$ . The whole diurnal cycle of the CLM-7.0 wind speed at the Mediterranean coast has a phase shift of 5 hr to the observations, which leads together with the high positive bias to a negative correlation coefficient of  $R = -0.6$  (not shown) and a high CRMSD ( $\text{CRMSD} > 3 \text{ m}\cdot\text{s}^{-1}$ ; Figure 10b). Due to the small number of data points for a case study, these statistical key numbers only serve for a qualitative approach. CLM-2.8 simulates the wind speed at the Mediterranean coast more realistically than CLM-7.0 (Figures 7f and 10b). The CLM-2.8 simulated diurnal cycle of the wind speed at the Mediterranean coast shows that its diurnal variation is

reproduced well apart from a slight overestimation and an average temporal shift of 2 hr (Figure 8b). The amplitudes of both observed wind speed maxima (A) and (B) are reproduced well (Figure 8b), while the simulated wind speed has a correlation coefficient of  $R = 0.2$  (Figure 10b), mainly caused by the time lag. Overall, the higher resolution simulation CLM-2.8 improves the estimate of the maximum wind speed, which is in agreement with Belušić *et al.* (2018).

Regarding ERA-5, it best reflects the wind speed on the Mediterranean coast on July 16, 2015 but with a significantly lower correlation coefficient of  $R = 0.36$  (Figure 10b) compared to the climatology ( $R = 0.70$ ; Figure 5b). The situation is completely different further inland. There, both at the Judean Mountains and the Dead Sea, the largest wind speeds are underestimated by up to  $6 \text{ m/s}$  at 2100 LST at the west coast of the Dead Sea (Figure 8d).

On July 16, 2015 both COSMO-CLM simulations reproduce the diurnal cycle of wind speed at the west coast of the Dead Sea very well (Figure 8d). The width of

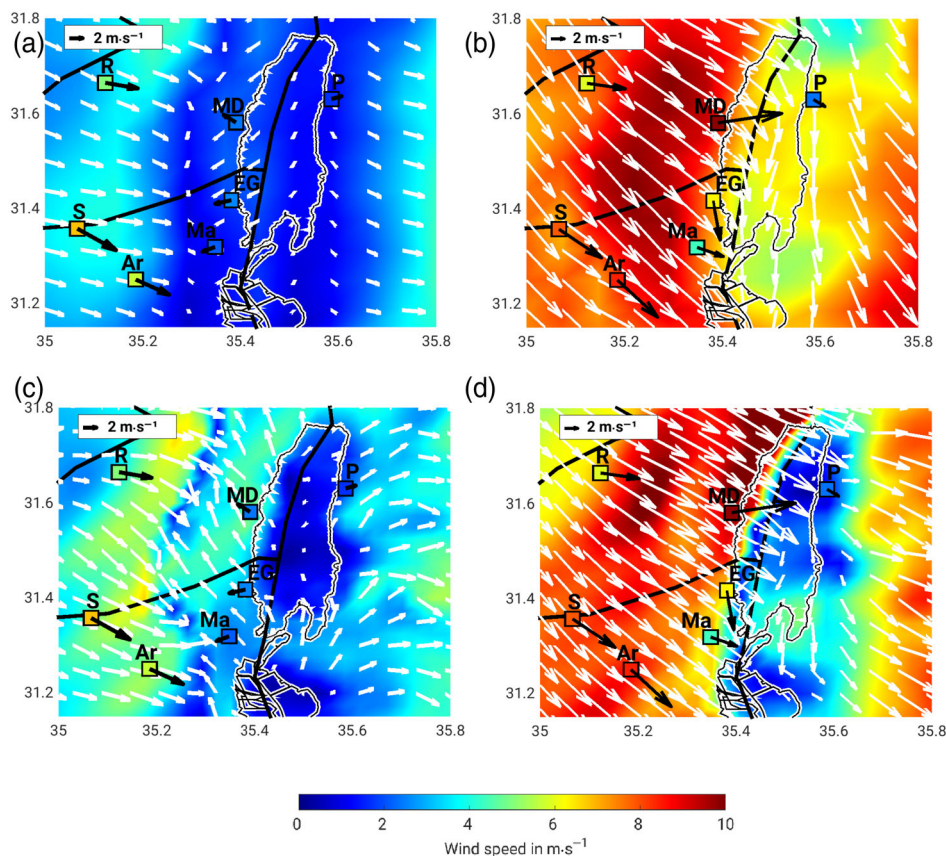


FIGURE 9 As Figure 7 only for the Dead Sea area and the CLM simulations [Colour figure can be viewed at [wileyonlinelibrary.com](https://onlinelibrary.wiley.com/doi/10.1002/joc.7695)]

the maximum in the diurnal cycle of wind speed is a bit better captured by CLM-2.8, confirming that sharp, short-duration events can also be better represented in terms of winds by higher resolution (Rummukainen, 2016). Phase and amplitude of both COSMO-CLM wind speed maxima agree with the observations (Figure 8d). The relative wind speed maximum at 0200 LST is not captured by the simulations. On this day, this relative wind maximum is produced by small-scale downslope winds on the eastern slopes of the Judean Mountains (Paperman *et al.*, 2021). This leads to correlation coefficients  $R > 0.8$  and  $CRMSD < 1.5 \text{ m} \cdot \text{s}^{-1}$  (Figure 10d). On the west coast of the Dead Sea, the differences in statistical properties for the two COSMO-CLM simulations are small (Figure 10d). But still the wind speed of the CLM-2.8 simulation achieves a higher correlation coefficient, a lower centered root-mean-square deviation, and a lower standard deviation difference than CLM-7.0.

Averaged over all observations, the CLM simulations and the ERA-5 reanalysis can reproduce the approximate course of the diurnal wind speed (Figure 8a). Both CLM simulations show a positive bias, especially in the afternoon and evening. Leaving aside the Mediterranean coast, the case-study Taylor diagrams show very similar metrics compared to the climatology (Figures 5 and 10).

However, the subarea analysis shows that the COSMO-CLM simulations are able to resolve the individual structure of the small-scale near-surface wind fields very well. And this is true also in areas with complex orography, such as the Jordan Rift valley or the Mediterranean coast, resulting in large improvements compared to the ERA-5 reanalysis (Figures 7 and 10d). As in the climatology, on July 16, 2015 the CLM-2.8 simulation reproduces wind speeds even better than the CLM-7.0 simulation, both on average over the entire area (Figure 10a) and for all sub-areas (Figure 10b–d). Again, the largest differences occur on the Mediterranean coast (Figures 6b,d, 7d,f, 8b and 10b).

In the eastern Mediterranean the near-surface wind field is similar to the selected case study for most summer days. Video S3 shows the near-surface wind field of CLM-2.8 for the period from July 11, 2015 to July 23, 2015. CLM-2.8 can reproduce the repeating interactions of the wind systems for the whole time period (Figure 1e,f). July 16, 2015 is an example for a long-range wind event. This case study and additional ones (not shown) confirm that for long range events, CLM-2.8 simulates more realistically the shape, timing and magnitude of the wind speed maximum at the west coast of the Dead Sea.

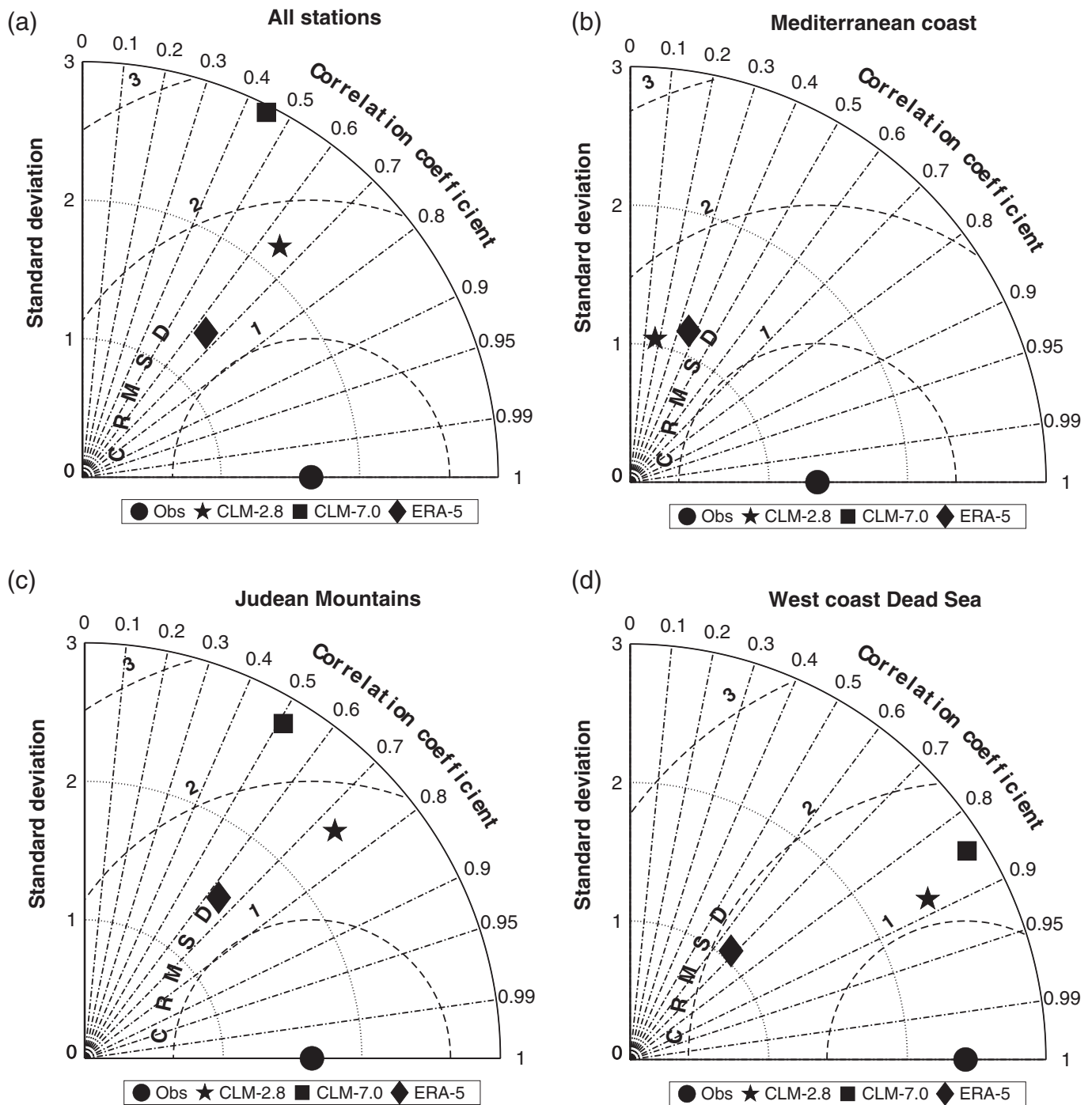


**FIGURE 10** Taylor diagrams (Taylor, 2001) for the evaluation of hourly wind speed between 0800 and 2200 LST on July 16, 2015 for the two CLM simulations and the ERA-5 reanalysis regarding 10 m height wind station observations (Obs) averaged for all stations (a), the Mediterranean coast (b), the Judean Mountains (c) and the west coast of the Dead Sea (d). Table 1 shows which stations belong to the different subareas

The range of the Mediterranean Sea breeze into the Jordan Rift valley is an important feature for the region as it strongly influences parameters such as wind, temperature and humidity at the Dead Sea (Vüllers *et al.*, 2018; Kunin *et al.*, 2019). Therefore, we further discuss August 3, 2015 as an example of a short-range

Mediterranean Sea breeze event. The realistic simulation of the near-surface wind field near the Dead Sea for short ranges is very challenging for both CLM simulations. The CLM-7.0 simulation overestimates wind speeds at the vicinity of the Dead Sea (Figure 11a). The CLM-2.8 simulation recognizes that the high wind speeds do not reach

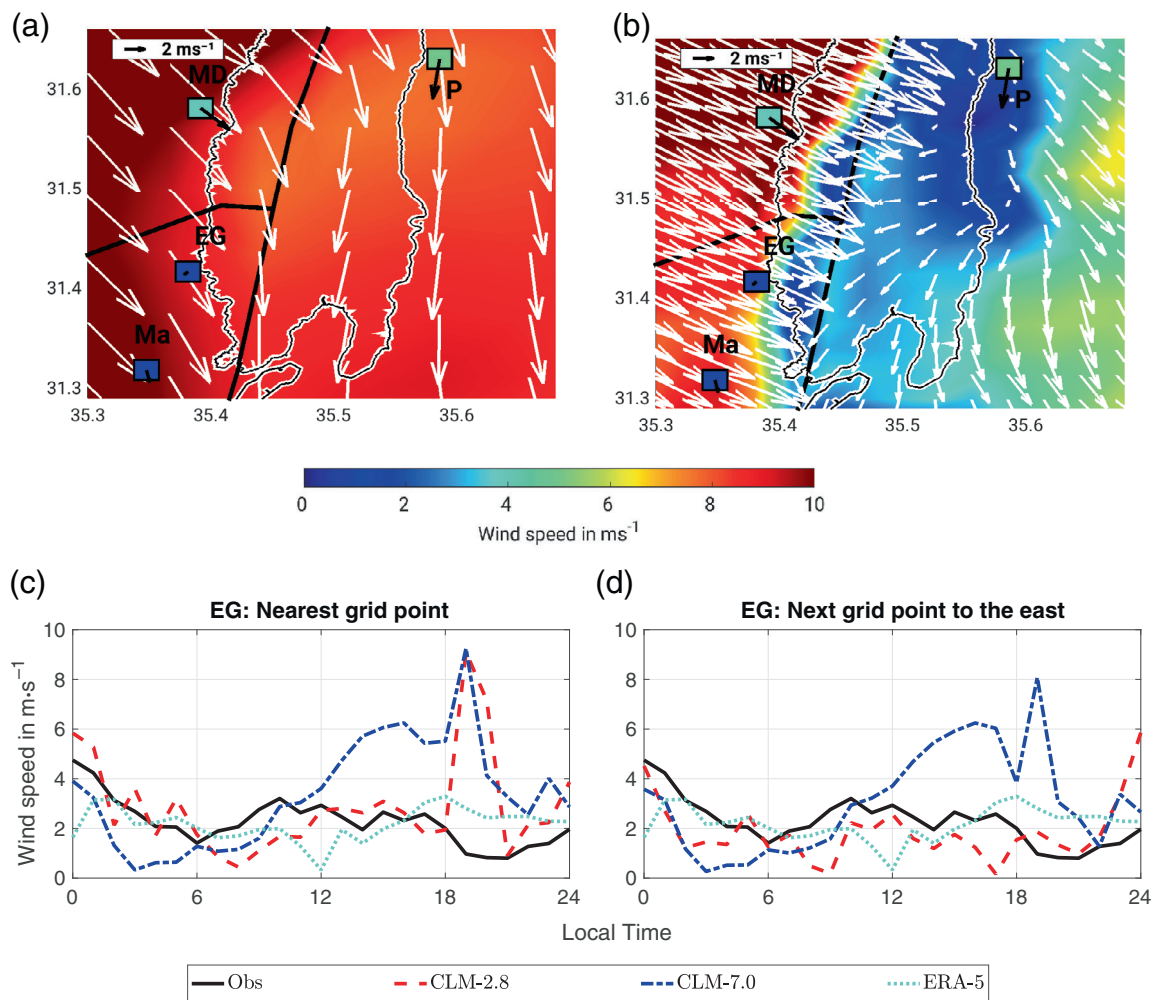


**FIGURE 11** As Figure 9 on August 3, 2015 for CLM-7.0 (a) and CLM-2.8 (b) at 1900 LST for a part of the Dead Sea area. Diurnal cycle of hourly averaged wind speed on August 3, 2015 of the wind station (Obs) and the nearest grid point (c) or the nearest grid point to the east (d) of the two CLM simulations and ERA-5 reanalysis for Ein Gedi (EG) at the west coast of the Dead Sea [Colour figure can be viewed at [wileyonlinelibrary.com](http://wileyonlinelibrary.com)]

over the Dead Sea (Figure 11b). This is an important information, because thus the winds in the Dead Sea valley are decoupled from the Mediterranean Sea breeze, which does not reach the valley. Therefore, the local sea breeze of the Dead Sea and the northerly winds along the valley dominate. However, the wind front is simulated too far east by CLM-2.8. This leads to an overestimation of  $\sim 8 \text{ m s}^{-1}$  at the west coast of the Dead Sea at 1900 LST in both simulations (Figure 11c). But if we compare the observations with the closest model grid point located to the east, improvements in the high-resolution simulation can indeed be identified (Figure 11d), as this grid point already is located behind the simulated wind front. For example, CLM-2.8 captures the weak wind speeds between 1800 and 2100 LST. At this time, there are strong small-scale wind speed gradients on the west coast of the Dead Sea. These small-scale structures are well captured by the CLM-2.8 simulation given a reasonable

choice of the reference grid point near the observation (east) or by averaging several surrounding grid points.

## 4 | SUMMARY AND CONCLUSIONS

The purpose of this paper is to evaluate the performance of high-resolution regional climate simulations in representing the climatology and the interaction of near-surface summer wind systems on individual days in the eastern Mediterranean. With this aim, we compare COSMO-CLM wind simulations at 2.8 and 7.0 km horizontal resolutions with IMS observations over the region, and a unique data set over the complex orography of the Dead Sea from KIT-DESERVE (section 2) both for climatology and two case studies in mid-summer 2015. The key conclusions are as follows:

1. The high-resolution COSMO-CLM simulations largely reproduce the main characteristics of the regional wind systems in the eastern Mediterranean, whereas ERA-5 is only able to represent the Mediterranean Sea breeze. The COSMO-CLM simulations reproduce the Mediterranean Sea breeze, the local Dead Sea breeze, the slope winds in the Judean Mountains and the winds along the Jordan Rift valley in both the climatology and the case studies. However, ERA-5 reanalysis only reproduces the Mediterranean Sea breeze with weak intensity (relative error median wind speed  $\text{ReMedian} = -24\%$ ) and weak standard deviation (relative error standard deviation wind speed  $\text{ReSD} = -31\%$ ), especially near the Dead Sea in the late afternoon. We therefore conclude that the other wind systems (slope winds, Dead Sea breeze) cannot be resolved at 31 km horizontal resolution due to the inaccurate representation of orography and land–sea distribution in ERA-5 (Zhu and Atkinson, 2004; Crosman and Horel, 2010). A horizontal resolution of a few km is required to capture small-scale wind systems (Belušić *et al.*, 2018).
  2. The high-resolution simulations qualitatively and quantitatively improve the representation of regional near-surface wind systems both for climatology and individual cases, particularly over complex orography. Indeed, we find added value in using higher resolution simulations for both climatology and the two case studies, which agrees with Akhtar *et al.* (2018). The influence of an increased model horizontal resolution on the simulation of near-surface wind fields depends on the large-scale weather pattern, the time of the day and the location. In general, the highest model resolution (2.8 km) provides more realistic near-surface wind fields in 88% of the days compared to a resolution of 7.0 km. The differences in reproducing wind speeds between the two simulations are largest in the afternoon and evening near the Dead Sea and near the Mediterranean coast. This is the time of day when horizontal temperature and pressure gradients are largest and small-scale features strongly influence wind systems. This improvement is largely related to the use of high-resolution terrain information in the model (GLOBE data set) simulating the complex orography of the Jordan Rift Valley. Along the Mediterranean coast, simulated wind speeds between CLM-7.0 and CLM-2.8 differ from each other even more than in the Jordan Rift valley due to differences in representing land–sea density gradients between both resolutions (2.8 and 7.0 km). Other improvements of reaching a convection-permitting resolution are that the positive bias in wind speed can be reduced by 34%. Furthermore, the time lag can be reduced. In the climatology the CLM-7.0 diurnal cycle of wind speed is delayed about 1.7 hr from observations. On individual days the delay can be more than 5 hr, particularly near the Mediterranean coast. The CLM-2.8 diurnal cycle is on average 1.1 hr late compared to observations, showing better results than CLM-7.0. Nevertheless, the use of a convection-permitting grid does not guarantee the accurate representation of near-surface wind for all days (also seen in Kunin *et al.*, 2019).
  3. Case studies show that only CLM-2.8 can reproduce daily small-scale interactions of the three prevailing wind systems in the region. Subdaily features like the extent of the Mediterranean Sea breeze into the Jordan Rift valley and the short-time variability of the near-surface wind field are more accurately reproduced by CLM-2.8. This is true also in areas with complex orography, such as the Jordan Rift valley or the Mediterranean coast, resulting in large improvements compared to coarser resolutions. Especially for long-range days (85% of days), CLM-2.8 shows improvements to capture the shape, timing and magnitude of the wind speed maximum near the west coast of the Dead Sea. Short-range events are more challenging for both CLM simulations. The higher resolution does show improvements on most days by simulating a frontal area with a strong wind speed gradient. However, this frontal area is simulated often too far to the east. Small-scale wind structures can be well captured by the CLM-2.8 simulation. Furthermore, secondary wind features like convergence lines and important flow structures can be resolved by CLM-2.8, which are not represented in a coarser resolution model. These important features are smoothed out in the climatology.
- Since the near-surface wind and particularly the Mediterranean Sea breeze have a strong influence on further meteorological parameters like temperature, humidity, turbulent heat fluxes (Akhtar *et al.*, 2018) and air quality (Kishcha *et al.*, 2016; Vüllers *et al.*, 2018; Kunin *et al.*, 2019), these variables accurate representation in a model is necessary to reproduce the main climatic features and their changes during summer (Alpert *et al.*, 1982; Hochman *et al.*, 2018a). A realistic reproduction of the wind field is also important for wind energy projections, fire management, public health and seasonal future planning purposes, for example, industry, traffic recreation areas under conditions of global climate change. In the coming years a realistic modelling of regional climate conditions by regional climate models will be even more relevant to determine the impacts of climate change at the local and regional scale (Jaeger *et al.*, 2008). Indeed, the eastern Mediterranean is expected to be particularly

affected by climate change (Shafir and Alpert, 2011; Lelieveld *et al.*, 2012; Hochman *et al.*, 2018c; 2022) leading to increasing temperatures and humidity. Regional wind systems like sea breezes, slope winds and winds along a valley are frequent phenomena that are important to modulate the regional changes in temperature and humidity, either easing or amplifying the warming effect. We therefore envisage that such high-resolution simulations are also required at other regions with complex orography for short and long-term analyses.

## ACKNOWLEDGEMENTS

This paper is a contribution to “The Hydrological cycle in the Mediterranean Experiment community” (HyMeX, <https://www.hymex.org/>) in close cooperation with the international virtual institute “Dead Sea Research Venue” (DESERVE, <https://www.imk-tro.kit.edu/10897.php>), funded by the Helmholtz Association of German Research Centers under No. VH-VI-527. The model simulations were performed on the computational resource ForHLR funded by the Ministry of Science, Research and Arts Baden-Württemberg and by “Deutsche Forschungsgemeinschaft.” M. R. Latt, A. Hochman and U. Corsmeier thank the German Helmholtz Association (“Changing Earth” program) for funding. J. G. Pinto thanks the AXA Research Fund (<https://www.axa-research.org/en/project/joaquim-pinto>) for support. The authors would like to acknowledge Eitan Campbell, former director of Masada National Park, Dead Sea, Israel and Yael Maor, General Director of Dead Sea – Arava Science Center, Israel for their generous support in establishing a meteorological network within DESERVE at the Dead Sea. Many thanks to the Israel Meteorological Service (IMS) for providing us with data of its synoptical network. A. Hochman thanks the Hebrew University of Jerusalem for technical assistance in maintaining the stations deployed in the Dead Sea region. We thank the reviewers for their valuable comments that helped to improve the manuscript. Open Access funding enabled and organized by Projekt DEAL.

## ORCID

Melissa R. Latt  <https://orcid.org/0000-0002-3661-0113>  
Assaf Hochman  <https://orcid.org/0000-0002-9881-1893>

## REFERENCES

- Akhtar, N., Brauch, J. and Ahrens, B. (2018) Climate 417 modeling over the Mediterranean Sea: impact of resolution and ocean coupling. *Climate Dynamics*, 51, 933–948.
- Alpert, P., Cohen, A., Neumann, J. and Doron, E. (1982) A model simulation of the summer circulation from the eastern Mediterranean past Lake Kinneret in the Jordan Valley. *Monthly Weather Review*, 110, 994–1006.
- Alpert, P. and Getenio, B. (1988) One-level diagnostic modeling of mesoscale surface winds in complex terrain. Part I: comparison with three-dimensional modeling in Israel. *Monthly Weather Review*, 116, 2025–2046.
- Alpert, P., Osetinsky, I., Ziv, B. and Shafir, H. (2004) A new seasons definition based on classified daily synoptic systems: an example for the eastern Mediterranean. *International Journal of Climatology*, 24, 1013–1021.
- Alpert, P. and Rabinovich-Hadar, M. (2003) Pre- and post-sea breeze frontal lines—a meso- $\gamma$ -scale analysis over south Israel. *Journal of the Atmospheric Sciences*, 60, 2994–3008.
- Asaf, D., Peleg, M., Alsawair, J., Soleiman, A., Matveev, V., Tas, E., Gertler, A. and Luria, M. (2011) Trans-boundary transport of ozone from the eastern Mediterranean coast. *Atmospheric Environment*, 45, 5595–5601.
- Ashbel, D. and Brooks, C. (1939) The influence of the Dead Sea on the climate of its neighbourhood. *Quarterly Journal of the Royal Meteorological Society*, 65, 185–194.
- Belušić, A., Prtenjak, M.T., Güttler, I., Ban, N., Leutwyler, D. and Schär, C. (2018) Near-surface wind variability over the broader Adriatic region: insights from an ensemble of regional climate models. *Climate Dynamics*, 50, 4455–4480.
- Bitan, A. (1974) The wind regime in the north-west section of the Dead Sea. *Archiv für Meteorologie, Geophysik und Bioklimatologie, Serie B*, 22, 313–335.
- Bitan, A. (1976) The influence of the special shape of the Dead Sea and its environment on the local wind system. *Archiv für Meteorologie, Geophysik und Bioklimatologie, Serie B*, 24, 283–301.
- Bitan, A. and Sa’Aroni, H. (1992) The horizontal and vertical extension of the Persian Gulf pressure trough. *International Journal of Climatology*, 12, 733–747.
- Bucchignani, E., Cattaneo, L., Panitz, H.-J. and Mercogliano, P. (2016) Sensitivity analysis with the regional climate model COSMO-CLM over the CORDEX-MENA domain. *Meteorology and Atmospheric Physics*, 128, 73–95.
- Cattaneo, L., Zollo, A., Bucchignani, E., Montesarchio, M., Manzi, M. and Mercogliano, P. (2012) Assessment of COSMO-CLM performances over Mediterranean area. *CMCC Research Paper*, 2012, 144.
- Christensen, J.H., Carter, T.R., Rummukainen, M. and Amanatidis, G. (2007) Evaluating the performance and utility of regional climate models: the PRUDENCE project. *Climate Change*, 81, 1–6.
- Crosman, E.T. and Horel, J.D. (2010) Sea and lake breezes: a review of numerical studies. *Boundary-Layer Meteorology*, 137, 1–29.
- Di Luca, A., de Elia, R. and Laprise, R. (2015) Challenges in the quest for added value of regional climate dynamical downscaling. *Current Climate Change Reports*, 1, 10–21.
- Diffenbaugh, N.S., Pal, J.S., Giorgi, F. and Gao, X. (2007) Heat stress intensification in the Mediterranean climate change hotspot. *Geophysical Research Letters*, 34, L11706.
- Doms, G., Förstner, J., Heise, E., Herzog, H.-J., Mironov, D., Raschendorfer, M., Reinhardt, T., Ritter, B., Schrodin, R., Schulz, J.-P. and Vogel, G. (2011) *A description of the non-hydrostatic regional COSMO model part II: physical parameterization*. Offenbach: German Weather Service.
- Drobinski, P., Alpert, P., Cavicchia, L., Flaounas, E., Hochman, A. and Kotroni, V. (2018a) Strong winds: observed trends, future

- projections. In: *The Mediterranean Region under Climate Change: A Scientific Update*. Marseille: IRD.
- Drobinski, P., Bastin, S., Arsouze, T., Beranger, K., Flaounas, E. and Stefanon, M. (2018b) North-western Mediterranean sea breeze circulation in a regional climate system model. *Climate Dynamics*, 51, 1077–1093.
- Evans, J.P., Smith, R.B. and Oglesby, R.J. (2004) Middle East climate simulation and dominant precipitation processes. *International Journal of Climatology*, 24, 1671–1694.
- Feser, F., Rockel, B., von Storch, H., Winterfeldt, J. and Zahn, M. (2011) Regional climate models add value to global model data: a review and selected examples. *Bulletin of the American Meteorological Society*, 92, 1181–1192.
- Giorgi, F., Jones, C., Asrar, G.R. (2009) Addressing climate information needs at the regional level: the CORDEX frame work. *World Meteorological Organization (WMO) Bulletin*, 58, 175.
- Goldreich, Y. (2012) *The Climate of Israel: Observation, Research and Application*. New York: Springer.
- Haslinger, K., Anders, I. and Hofstätter, M. (2013) Regional climate modelling over complex terrain: an evaluation study of COSMO-CLM hindcast model runs for the Greater Alpine Region. *Climate Dynamics*, 40, 511–529.
- Hecht, A. and Gertman, I. (2003) Dead Sea meteorological climate. In: *Fungal life in the Dead Sea*. Haifa, Israel: International Center for Cryptogamic Plants and Fungi, Institute of Evolution, University of Haifa, pp. 68–114.
- Hersbach, H., Bell, B., Berrisford, P., Hirahara, S., Horányi, A., Muñoz-Sabater, J., Nicolas, J., Peubey, C., Radu, R., Schepers, D., Simmons, A., Soci, C., Abdalla, S., Abellan, X., Balsamo, G., Bechtold, P., Biavati, G., Bidlot, J., Bonavita, M., Chiara, G., Dahlgren, P., Dee, D., Diamantakis, M., Dragani, R., Flemming, J., Forbes, R., Fuentes, M., Geer, A., Haimberger, L., Healy, S., Hogan, R.J., Hólm, E., Janisková, M., Keeley, S., Laloyaux, P., Lopez, P., Lupu, C., Radnoti, G., Rosnay, P., Rozum, I., Vamborg, F., Villaume, S. and Thépaut, J.N. (2020) The ERA5 global reanalysis. *Quarterly Journal of the Royal Meteorological Society*, 146, 1999–2049.
- Hochman, A., Buchignani, E., Gershtein, G., Krichak, S.O., Alpert, P., Levi, Y., Yosef, Y., Carmona, Y., Breitgand, J., Mercogliano, P. and Zollo, A.L. (2018a) Evaluation of regional COSMO-CLM climate simulations over the eastern Mediterranean for the period 1979–2011. *International Journal of Climatology*, 38, 1161–1176.
- Hochman, A., Harpaz, T., Saaroni, H. and Alpert, P. (2018b) The seasons length in 21st century CMIP5 projections over the eastern Mediterranean. *International Journal of Climatology*, 38, 2627–2637.
- Hochman, A., Marra, F., Messori, G., Pinto, J.G., Raveh-Rubin, S., Yosef, Y. and Zittis, G. (2022) Extreme weather and societal impacts in the eastern Mediterranean. *Earth System Dynamics*, 13, 749–777.
- Hochman, A., Mercogliano, P., Alpert, P., Saaroni, H. and Buchignani, E. (2018c) High-resolution projection of climate change and extremity over Israel using COSMO-CLM. *International Journal of Climatology*, 38, 5095–5106.
- Hochman, A., Scher, S., Quinting, J., Pinto, J.G. and Messori, G. (2021) A new view of heat wave dynamics and predictability over the eastern Mediterranean. *Earth System Dynamics*, 12, 133–149.
- Jaeger, E.B., Anders, I., Luthi, D., Rockel, B., Schar, C. and Seneviratne, S.I. (2008) Analysis of ERA40-driven CLM simulations for Europe. *Meteorologische Zeitschrift*, 17, 349–368.
- Kendon, E.J. (2014) Very high resolution regional climate modeling—benefits and future prospects. In: *21st Century Challenges in Regional Climate Modelling*, Geesthacht: 3rd Lund Regional-scale Climate Modelling Workshop; Vol. 136, p. 118.
- Kishcha, P., Starobinets, B. and Alpert, P. (2016) Modeling of foehn-induced extreme local dust pollution in the Dead Sea valley. In: *International Technical Meeting on Air Pollution Modelling and its Application*. Cham: Springer, pp. 433–437.
- Kotlarski, S., Bosshard, T., Lüthi, D., Pall, P. and Schär, C. (2011) Elevation gradients of European climate change in the regional climate model COSMO-CLM. *Climatic Change*, 112, 1–27.
- Kotlarski, S., Keuler, K., Christensen, O.B., Colette, A., Déqué, M., Gobiet, A., Goergen, K., Jacob, D., Lüthi, D., Van Meijgaard, E., et al. (2014) Regional climate modeling on European scales: a joint standard evaluation of the EURO-CORDEX RCM ensemble. *Geoscientific Model Development*, 7, 1297–1333.
- Kottmeier, C., Agnon, A., Al-Halbouni, D., Alpert, P., Corsmeier, U., Dahm, T., Eshel, A., Geyer, S., Haas, M., Holohan, E., et al. (2016) New perspectives on interdisciplinary earth science at the Dead Sea: the DESERVE project. *Science of the Total Environment*, 544, 1045–1058.
- Kunin, P., Alpert, P. and Rostkier-Edelstein, D. (2019) Investigation of sea-breeze/foehn in the Dead Sea valley employing high resolution WRF and observations. *Atmospheric Research*, 229, 240–254.
- Kusuda, M. and Alpert, P. (1983) Anti-clockwise rotation of the wind hodograph. Part I: theoretical study. *Journal of Atmospheric Sciences*, 40, 487–499.
- Lelieveld, J., Hadjinicolaou, P., Kostopoulou, E., Chenoweth, J., El Maayar, M., Giannakopoulos, C., Hannides, C., Lange, M., Tanarhte, M., Tyrllis, E., et al. (2012) Climate change and impacts in the eastern Mediterranean and the Middle East. *Climatic Change*, 114, 667–687.
- Levi, Y., Shilo, E. and Setter, I. (2011) Climatology of a summer coastal boundary layer with 1290-MHz wind profiler radar and aWRF simulation. *Journal of Applied Meteorology and Climatology*, 50, 1815–1826.
- Mellor, G.L. and Yamada, T. (1974) A hierarchy of turbulence closure models for planetary boundary layers. *Journal of Atmospheric Sciences*, 31, 1791–1806.
- Metzger, J. (2017) *Wind Systems and Energy Balance in the Dead Sea Valley*, Vol. 74. Karlsruhe: KIT Scientific Publishing.
- Moemken, J., Feldmann, H., Pinto, J.G., Buldmann, B., Laube, N., Kadow, C., Paxian, A., Tiedje, B., Kottmeier, C. and Marotzke, J. (2021) The regional MiKlip decadal prediction system for Europe: Hindcast skill for extremes and user-oriented variables. *International Journal of Climatology*, 41, E1944–E1958.
- Naor, R., Potchter, O., Shafir, H. and Alpert, P. (2017) An observational study of the summer Mediterranean Sea breeze front penetration into the complex topography of the Jordan Rift Valley. *Theoretical and Applied Climatology*, 127, 275–284.
- Nolan, P., Lynch, P., McGrath, R., Semmler, T. and Wang, S. (2014) Simulating climate change and its effects on the wind energy resource of Ireland. *Wind Energy*, 15, 593–608.

- Önol, B. and Semazzi, F.H.M. (2009) Regionalization of climate change simulations over the eastern Mediterranean. *Journal of Climate*, 22, 1944–1961.
- Panitz, H.-J., Dosio, A., Büchner, M., Lüthi, D. and Keuler, K. (2014) COSMO-CLM (CCLM) climate simulations over CORDEX Africa domain: analysis of the ERA-Interim driven simulations at 0.44 and 0.22 resolution. *Climate Dynamics*, 42, 3015–3038.
- Papanastasiou, D.K., Melas, D., Bartzanas, T. and Kittas, C. (2010) Temperature, comfort and pollution levels during heat waves and the role of sea breeze. *International Journal of Biometeorology*, 54, 307–317.
- Paperman, J., Potchter, O. and Alpert, P. (2021) Characteristics of the summer 3-D katabatic flow in a semi-arid zone—The case of the Dead Sea. *International Journal of Climatology*, 42, 1975–1984.
- Prein, A., Gobiet, A., Suklitsch, M., Truhetz, H., Awan, N., Keuler, K. and Georgievski, G. (2013) Added value of convection permitting seasonal simulations. *Climate Dynamics*, 41, 2655–2677.
- Prein, A.F., Langhans, W., Fosser, G., Ferrone, A., Ban, N., Goergen, K., Keller, M., Tölle, M., Gutjahr, O., Feser, F., Brisson, E., Kollet, S., Schmidli, J., Lipzig, N.P.M. and Leung, R. (2015) A review on regional convection-permitting climate modeling: demonstrations, prospects, and challenges. *Reviews of Geophysics*, 53, 323–361.
- Ramon, J., Lledo, L., Torralba, V., Soret, A. and Doblas-Reyes, F.J. (2019) What global reanalysis best represents near-surface winds? *Quarterly Journal of the Royal Meteorological Society*, 145, 3236–3251.
- Ritter, B. and Geleyn, J.-F. (1992) A comprehensive radiation scheme for numerical weather prediction models with potential applications in climate simulations. *Monthly Weather Review*, 120, 303–325.
- Rockel, B., Will, A. and Hense, A. (2008) The regional climate model COSMO-CLM (CCLM). *Meteorologische Zeitschrift*, 17, 347–348.
- Rummukainen, M. (2010) State-of-the-art with regional climate models. *Wiley Interdisciplinary Reviews: Climate Change*, 1, 82–96.
- Rummukainen, M. (2016) Added value in regional climate modeling. *Wiley Interdisciplinary Reviews: Climate Change*, 7, 145–159.
- Schättler, U., Doms, G. and Schraff, C. (2016) *A description of the nonhydrostatic regional COSMO-model, part VII: user's guide*. Offenbach: Deutscher Wetterdienst.
- Shafir, H. and Alpert, P. (2011) Regional and local climatic effects on the Dead-Sea evaporation. *Climatic Change*, 105, 455–468.
- Shafir, H., Jin, F., Lati, Y., Cohen, M. and Alpert, P. (2008) Wind channeling by the Dead-Sea wadis. *Open Atmospheric Science Journal*, 2, 139–152.
- Steinberger, E. (1980) Transport of ozone in Israel. In: *Studies in Environmental Science*, Vol. 8. Amsterdam and New York: Elsevier, pp. 165–171.
- Taylor, K.E. (2001) Summarizing multiple aspects of model performance in a single diagram. *Journal of Geophysical Research: Atmospheres*, 106, 7183–7192.
- Tiedtke, M. (1989) A comprehensive mass flux scheme for cumulus parameterization in large-scale. *Monthly Weather Review*, 117, 1779–1800.
- Vautard, R., Gobiet, A., Jacob, D., Belda, M., Colette, A., Déqué, M., Fernández, J., García-Diez, M., Goergen, K., Güttler, I., Halenka, T., Karacostas, T., Katragkou, E., Keuler, K., Kotlarski, S., Mayer, S., van Meijgaard, E., Nikulin, G., Patarčić, M., Scinocca, J., Sobolowski, S., Suklitsch, M., Teichmann, C., Warrach-Sagi, K., Wulfmeyer, V. and You, P. (2013) The simulation of European heat waves from an ensemble of regional climate models within the EURO-CORDEX project. *Climate Dynamics*, 41, 2555–2575.
- Vüllers, J., Mayr, G.J., Corsmeier, U. and Kottmeier, C. (2018) Characteristics and evolution of diurnal foehn events in the Dead Sea valley. *Atmospheric Chemistry and Physics*, 18, 18169–18186.
- Zardi, D. and Whiteman, C.D. (2013) Diurnal mountain wind systems. In *Mountain Weather Research and Forecasting* (pp. 35–119). Dordrecht: Springer. [https://doi.org/10.1007/978-94-007-4098-3\\_2](https://doi.org/10.1007/978-94-007-4098-3_2)
- Zhou, W., Tang, J., Wang, X., Wang, S., Niu, X. and Wang, Y. (2016) Evaluation of regional climate simulations over the CORDEX EA-II domain using the COSMO-CLM model. *Asia-Pacific Journal of Atmospheric Sciences*, 52, 107–127.
- Zhu, M. and Atkinson, B. (2004) Observed and modelled climatology of the land-sea breeze circulation over the Persian Gulf. *International Journal of Climatology*, 24, 883–905.
- Ziv, B., Saaroni, H. and Alpert, P. (2004) The factors governing the summer regime of the eastern Mediterranean. *International Journal of Climatology*, 24, 1859–1871.
- Zollo, A.L., Rillo, V., Bucchignani, E., Montesarchio, M. and Mercogliano, P. (2016) Extreme temperature and precipitation events over Italy: assessment of high-resolution simulations with COSMO-CLM and future scenarios. *International Journal of Climatology*, 36, 987–1004.

## SUPPORTING INFORMATION

Additional supporting information may be found in the online version of the article at the publisher's website.

**How to cite this article:** Latt, M. R., Hochman, A., Caldas-Alvarez, A., Helgert, S., Pinto, J. G., & Corsmeier, U. (2022). Understanding summer wind systems over the eastern Mediterranean in a high-resolution climate simulation. *International Journal of Climatology*, 1–20. <https://doi.org/10.1002/joc.7695>